

# Improved Precipitation Rates and Data Quality by Using Polarimetric Measurements

Anthony Illingworth

Dept of Meteorology, University of Reading, Reading, RG6 6BB, UK

## 1 Introduction

The additional information provided by polarisation diversity radar has the potential to remove many of the ambiguities and uncertainties present when only the conventional reflectivity ( $Z$ ) and Doppler information are available. In this chapter we emphasise the application in an operational environment with a typical one degree beamwidth radar and a dwell time of about one sixth of a second so that it completes a PPI every minute and provides rainfall estimates with a spatial resolution of 2km or better. An excellent and very comprehensive book on polarimetric Doppler weather radar has recently appeared by Bringi and Chandrasekar (2001) and we refer the reader to this book for detailed derivations and analysis which we will simply quote. Essentially, polarimetric radar provides information on the shape and orientation of the radar targets. In section 2 we define the polarisation parameters, summarise their applications and discuss the theoretical and practical limits to the accuracy with which they can be estimated. The variation of raindrop shape with size and the typical raindrop size spectra are reviewed in section 3. The following sections consider how to exploit the shape and orientation information from a polarimetric radar which can transmit and receive horizontally and vertically polarised radiation as described by Gekat et al. (2003, this book).

- *Recognition of anomalous propagation and ground clutter (Section 4).*  
Precipitation particles are essentially an array of quasi-spherical scatterers which are usually small enough to Rayleigh scatter and so can be distinguished from ground echoes. Ground clutter and ‘anaprop’ are essentially non-Rayleigh scatterers and are far from spherical having very different scattering cross sections for horizontally and vertically polarised radiation.
- *Improved rainrate estimates ( $R$ ) when rain alone is present (Section 5).*  
Empirical  $Z(R)$  relationships of the form  $Z = aR^b$  result in errors of  $R$  of up to a factor of two. They arise because of the variability in the raindrop size spectrum:  $Z = \sum ND^6$  for rain, where  $N$  is the concentration and  $D$  the raindrop diameter, but  $R \simeq \sum ND^{3.67}$ . Because raindrops are oblate to a degree which depends upon their size, polarisation observations have the potential to estimate mean raindrop size and so provide better rainrates.
- *The use of combined and integral polarisation parameters (Section 6).*  
High resolution polarisation parameters tend to be very noisy. An alternative approach is to exploit their path integrated properties which can be

estimated much more accurately and use them as a constraint to provide, for example, absolute calibration of the radar reflectivity, an estimate of the constant ‘ $a$ ’ in  $Z = aR^b$ , and a measure of the attenuation.

- *Improved rainfall estimates when ice is present (Section 7).*  
Large hailstones lead to very high values of  $Z$  which can be interpreted as spuriously high rainfall rates, but may be identified because they are oblate and tend to tumble as they fall. Melting snowflakes are responsible for the enhanced radar return at the melting layer known as ‘the bright band’ and can easily be recognised because they are wet, oblate and fall with a characteristic rocking motion.
- *Correction for attenuation (Section 8).*  
Attenuation for the C-band (5.6cm wavelength) radars used in Europe and Japan is a serious problem in heavy rain. Polarisation parameters which are immune to attenuation can be used to correct for such effects.
- *Identification of hydrometeors (Section 9).*  
For ice hydrometeors other than hail and melting snow, identification using polarisation is more difficult but polarisation can yield useful information.

In Section 10 the potential for implementation of polarisation parameters is summarised for an operational environment both for the 5.6cm wavelength (C-band) as generally used in Europe and Japan and 10cm (S-band) used in the USA. The use of S-band for polarisation observations has two major advantages: firstly, we have Rayleigh scattering for nearly all meteorological targets, and secondly, there are normally negligible propagation or attenuation problems. Conventional radar networks yield estimates of  $Z$  and rainfall rate with a spatial resolution of about 2km and an update time of 5 (or perhaps two and a half) minutes. If polarisation techniques require longer dwell times then the poor sampling could negate any increased accuracy of specific rainfall estimates.

## 2 The Polarisation Parameters

### 2.1 Introduction

We shall restrict the discussion to the use of linear polarisation in which the radar can transmit pulses which are alternately polarised in the horizontal ( $H$ ) and vertical ( $V$ ), and can measure both the two co-polar returns  $Z_H$ ,  $Z_V$ ; and, if the radar is Dopplerised, the phase of the horizontally and vertically polarised returns,  $\phi_h$  and  $\phi_v$ . We shall consider the following four parameters: the differential reflectivity ( $Z_{DR}$ ), the co-polar correlation ( $\rho_{hv}$ ), specific differential phase shift ( $K_{DP}$ ), and the linear depolarisation ratio (LDR). In principle, these four parameters can also be derived from measurements made with circular polarisation but nearly all recent work has used linear polarisation. We will also briefly discuss transmission of pulses polarised at  $45^\circ$  with reception at H and V, which has the advantage that no rapid polarisation switching between transmitted pulses is needed.

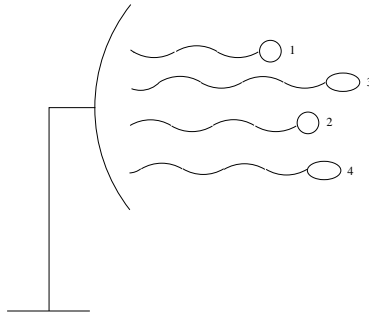


**Fig. 1.** Signals backscattered from precipitation particles arrive at the antenna with random phase.

Recall from Fig. 1, that the amplitudes of the backscattered waves from individual hydrometeors arrive at the antenna with random phase, so that as the scatterers move relative to one another, the observed intensity  $Z$  will fluctuate. The fractional standard error of the mean  $Z$  estimate is given by  $1/\sqrt{n}$  for large  $n$ , where  $n$  is the number of independent samples of  $Z$ . The time to independence is given by  $\lambda/(4\sigma_v\sqrt{\pi})$  where  $\sigma_v$  is the Doppler width of the target. Assuming that at a low beam elevation the precipitation has a Doppler width of  $0.5\text{m s}^{-1}$ , then the time to independence at C-band is about 16ms, and at S-band about 28ms. If we need one PPI a minute then the dwell time is 0.166s and averaging over six adjacent gates, each typically 150m long ( $1\mu\text{s}$  transmitted pulse), provides a range resolution of 1km to match the one degree beamwidth azimuthal resolution at a range of 57km. This leads to  $n$  of about 63 at C-band and 36 at S-band, so the statistical sampling error of  $Z$  will be about 13% (0.53dB) and 17% (0.68dB), respectively. System errors are discussed by Gekat et al. (2003, this book).

## 2.2 $Z_{DR}$ - Differential Reflectivity

$Z_{DR}$  ( $=10 \log(Z_H/Z_V)$ ) is a measure of mean particle shape.  $Z_{DR}$  is particularly useful for rain, because small raindrops are spherical but larger ones become increasingly oblate. An improved rainfall rate,  $R(Z, Z_{DR})$ , can be obtained from  $Z$  and  $Z_{DR}$ . Assuming an exponential Marshall-Palmer (1948) raindrop size distribution

$$N(D) = N_0 \exp(-3.67D/D_0) \quad (1)$$

where  $D_0$  is the median volume drop diameter, then the value of  $D_0$  can be estimated from  $Z_{DR}$ . The advantage of  $Z_{DR}$  is that it is a ratio which is independent of the concentration parameter,  $N_0$ . Once  $D_0$  is known then the value of  $N_0$  is fixed by the observed value of  $Z$ . An empirical  $Z$ - $R$  relationship is approximately equivalent to assuming we have a Marshall-Palmer distribution with a variable  $D_0$  but  $N_0$  constant and equal to  $8000 \text{ m}^{-3} \text{ mm}^{-1}$ . The use of  $Z$  and  $Z_{DR}$  to fix both  $N_0$  and  $D_0$  should result in more accurate rainfall estimates (Seliga and

Bringi, 1976). For a given value of  $Z_{DR}$  (fixed  $D_0$ ), the rainfall rate and the value of  $Z$  both scale linearly with  $N_0$ , so we expect relationships of the form:

$$Z = cRf(Z_{DR}) \quad (2)$$

Ice particles have a lower dielectric constant than liquid water and so even if they are oblate they tend to have low values of  $Z_{DR}$ , particularly if, as is the case of snow, they are a low density mixture of air and ice. If oblate ice particles become wet, the value of  $Z_{DR}$  increases, and so the melting snow in the bright band is associated with high values of  $Z_{DR}$ . In vigorous convection supercooled raindrops can be recognised by narrow vertical columns of positive  $Z_{DR}$  extending above the freezing level (e.g. Illingworth et al., 1987). Hail usually tumbles as it falls and so should be associated with a  $Z_{DR}$  of 0dB. At low altitudes, where rain is to be expected, a  $Z_{DR}$  value of 0dB accompanied by a high value of  $Z$  can be used to identify hail. Unfortunately, hail is often mixed with rain - so the result will be an intermediate value of  $Z_{DR}$ , which is lower than it should be for the rain, but the presence of hail will lead to higher than expected values of  $Z$ . In section 5 we shall show that for improved rainfall estimates using  $R(Z, Z_{DR})$ ,  $Z$  must be accurately calibrated and  $Z_{DR}$  estimated to within 0.2dB.  $Z_{DR}$  can be calibrated to 0.1dB by observing precipitation at vertical incidence which we know has a value of 0dB, or, less satisfactorily, looking at the statistics of  $Z_{DR}$  values in very light drizzle. Bringi et al. (1983) show that for individual observations to be accurate to 0.2dB requires about 60 independent samples of  $Z$  and a correlation coefficient of the  $H$  and  $V$  time series (see next subsection) above 0.98. These values should be satisfied by an operational radar scanning in rain with a resolution of about 1-2km, but in practice other factors may limit the accuracy of  $Z_{DR}$ :

- *Reflectivity Gradients.*

In the presence of reflectivity gradients a significant fraction of the power may be received through the sidelobes which are mismatched in their polarisation characteristics. Herzegh and Carbone (1984) report spurious values of  $Z_{DR}$  of up to 10dB in low reflectivity regions adjacent to intense echoes. The sidelobes of operational radars may well quite commonly lead to the introduction of errors in  $Z_{DR}$  of 0.2–0.5dB.

- *Mismatched beams.*

If the  $H$  and  $V$  beam patterns are not well matched then the two beams will not be sampling the same volume of precipitation and the correlation may fall below 0.98.

- *Triple scattering echoes.*

Triple scattering echoes (Illingworth and Caylor, 1988; Hubbert and Bringi, 2000) can occur in a weak echo region behind an intense storm because some of the radiation scattered by the main echo is reflected by the ground and then scattered a third time by the main echo back to the antenna. No vertically polarised power is scattered to the ground, so such echoes are associated with anomalously high values of  $Z_{DR}$ .

- *Differential attenuation.*

This leads to a much more severe problem at C-band. The large oblate raindrops attenuate the horizontally polarised radar beam more than the vertical one, and this differential attenuation leads to increasingly negative values of  $Z_{DR}$  with range. One example is shown by Collier and Hardacre (2003, this book). To demonstrate the severity of this problem, note that at C-band a differential attenuation of 0.2dB results from only 1km of rain at  $65 \text{ mm hr}^{-1}$  or 2km of rain at  $40 \text{ mm hr}^{-1}$ . Upton and Fernandez-Duran (1999) report values as low as  $-5\text{dB}$  behind intense echoes, such attenuation must be corrected to an accuracy of 0.2dB.

- *Hail.*

Finally, as described above, the presence of hail mixed with the rain will lead to a reduction in  $Z_{DR}$  so that application of the  $R(Z, Z_{DR})$  algorithm will lead to the inference of a spuriously high rainfall rate.

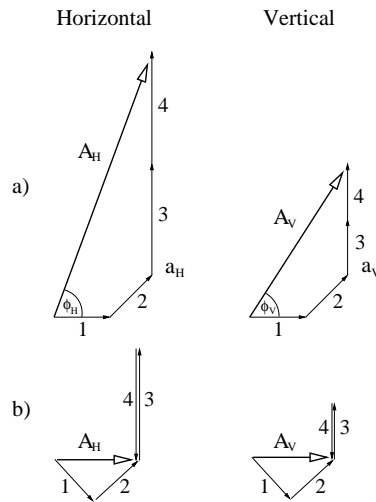


**Fig. 2.** Argand diagram showing that the addition of backscattered amplitudes from the mixture of particles shapes in Fig. 1, a) at time  $t=t_1$  and b) at a later time  $t=t_2$ , leads to a lowering of the correlation of the H and V returns and fluctuations in the differential phase.

### 2.3 Co-polar Correlation Coefficient

The co-polar correlation coefficient ( $\rho_{hv}$ ) is the correlation of the time series of successive estimates of  $Z_H$  and  $Z_V$  and is a measure of the variety of shapes of hydrometeors present. The importance of this parameter is demonstrated in Fig. 2 which shows schematically how the amplitude and phase of the signal

returned from four targets, two spheres and two oblate spheroids (see Fig. 1), add to give a fluctuating return as the targets reshuffle in space between two times,  $t=t_1$ , and  $t=t_2$ . In the figure the spheres and the oblate spheroids all have the same backscatter amplitude ( $a_v$ ) for vertical polarisation, but for horizontal polarisation the spheres have  $a_h = a_v$  whilst for the oblate spheroids  $a_h = 2a_v$ . The figure shows that as the particles reshuffle, the relative phases change and the resultant amplitudes  $A_h$  and  $A_v$  at the two polarisations will fluctuate. In this case because the ratio of  $a_h$  to  $a_v$  is not the same for all the scatterers, then as the particles reshuffle the ratio of  $A_h$  to  $A_v$  will fluctuate and so the time series of  $Z_H$  and  $Z_V$  (proportional to  $A_h^2$  and  $A_v^2$ ) will not be perfectly correlated. As the correlation falls then the estimate of  $Z_{DR}$  also becomes less accurate. The correlation coefficient, ( $\rho_{hv}$ ), will only be unity if the ratio of  $a_h$  to  $a_v$  is the same for all the particles, that is to say the particles all have the same shape and orientation in space. The values of correlation can be used to identify targets as follows:

- *Raindrops*  
Raindrops are nearly spherical and so the correlation is at least 0.98.
- *Hail and the Bright Band*  
The correlation drops to about 0.9 when a wide mixture of hydrometeor shapes is present. This occurs in the bright band or when hail particles are large enough to result in non-Rayleigh scattering.
- *Clutter and Anaprop*  
Returns from the ground, whether as clutter or anomalous propagation, have a correlation which is essentially zero because the returns in the two polarisations have almost random amplitudes and phases.

In practice the observed values of  $\rho_{hv}$  will be lowered somewhat because the  $H$  and  $V$  beams can never be perfectly matched in space and also because  $H$  and  $V$  are not sampled simultaneously. The effect of staggered  $H$  and  $V$  samples can be corrected by either assuming a Gaussian Doppler width of the target or, more accurately, by interpolating the two time series. For very precise estimates of  $\rho_{hv}$  the dwell times must be much longer than those allowed in an operational system. (Illingworth and Caylor, 1991).

#### 2.4 $K_{DP}$ - Specific Differential Phase.

The velocity of a horizontally polarised radar wave propagating through a region containing oblate raindrops is slightly less than that of a vertically polarised wave, so, as shown in Fig. 3, the phase of the horizontal return ( $\phi_h$ ) lags progressively behind the phase of the vertical polarised return ( $\phi_v$ ). As a result the differential phase,  $\phi_v - \phi_h = \phi_{DP}$ , normally increases monotonically with range and  $K_{DP}$ , the rate of change of  $\phi_{DP}$  with range (measured in  $^\circ \text{ km}^{-1}$ ), should be positive.  $K_{DP}$  should not be affected by tumbling hailstones, but should increase with rain rate.  $R(K_{DP})$  relationships (Sachidananda and Zrnica, 1986, 1987) have been proposed of the form:

$$R = aK_{DP}^b \quad (3)$$

with a value of  $b = 0.866$ . This technique appears to be very attractive, and has the following advantages (e.g., Blackman and Illingworth, 1995; Ryzhkov and Zrnic, 1996)

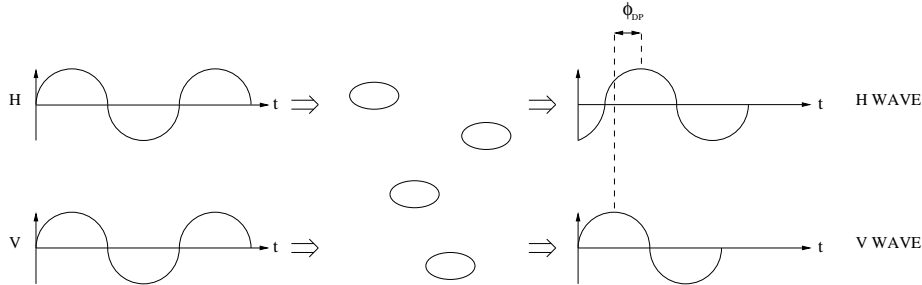


**Fig. 3.** Differential phase shift,  $\phi_{DP}$ , introduced because the H wave propagates more slowly than the V wave through a region of oblate raindrops.

- *Calibration and Attenuation*

The measurement of phase is immune to calibration problems and is unaffected by attenuation.

- *Hail*

The phase measurement should not be affected by hail.

- *Linearity*

If the value of 'b' in Eqn 3 is 0.866 then  $K_{DP}$  has a more linear dependence on  $R$  than conventional  $R(Z)$  relations. Bringi and Chandrasekar (2001) show that  $K_{DP}$  should be less dependent upon the precise form of the drop shapes and, assuming Rayleigh scattering, is approximately proportional to the product of the liquid water content times  $D_0$ , or to the fourth moment of the drop size spectrum and so should be closer to  $R$  than  $Z$ .

- *Integrated rainfall over a catchment.*

If Eqn 3 is nearly linear then the total integrated differential phase shift along the path of the radar beam ( $\Phi_{DP}$ ) will be a measure of the integrated rainfall along the path.

- *Use of partially blocked beams.*

If  $\phi_{DP}$  can be observed in low elevation beams which are partially blocked so that  $Z$  values are considerably reduced, it may be possible to estimate  $R$  from  $K_{DP}$  and so use these low elevations beams which will remain in the rain out to greater distances.

A difficulty arises because the phase shifts are quite small. If these advantages are to be realised, then  $\phi_{DP}$  should be estimated to  $1^\circ$  or better, but unfortunately the phase measurement can be quite noisy. Firstly, there is a theoretical limit to the accuracy of the  $\phi_{DP}$  estimate:

- *Sequential Pulses*

$\phi_{DP}$  is usually measured from sequential pulses transmitted with alternate horizontal and vertical polarisation, but the phase itself is continually changing due to the mean Doppler velocity of the targets and so interpolation is required to estimate  $\phi_{DP}$ . The accuracy of this interpolation is limited by the Doppler width of the target. Ryzhkov and Zrnich (1998b) show that for 60 pulse pairs and a normalised spectral width ( $= 2\sigma_v t_s / \lambda$ , where  $t_s$  is the time between pulses) of 0.1, the standard error of  $\phi_{DP}$ , ( $\sigma_\phi$ ), should be about  $1^\circ$ .

- *'Hybrid' Transmission at  $45^\circ$*

Transmission of a pulse polarised at  $45^\circ$  and simultaneous reception at  $H$  and  $V$  (Bringi and Chandrasekar, 2001) avoids the interpolation problem, but the correlation of the target is slightly less than unity and this introduces noise into the  $\phi_{DP}$  estimate which still leads to a  $\sigma_\phi$  of about  $1^\circ$ . The mechanism by which fluctuations in the estimate of  $\phi_{DP}$  are introduced by the low correlation can be seen in Fig. 2.

This theoretical accuracy of  $\phi_{DP}$  is not achieved in practice. Ryzhkov and Zrnich (1995) cite a typical  $\sigma_\phi$  at S-band of  $3^\circ$ , Hubbert et al. (1993) and Keenen et al. (1998) quote similar figures for their C-band radars. This degradation is probably caused by the following factors:

- *Gradients of reflectivity.*

Gradients in reflectivity across the beam cause one part of the beam to experience a larger  $\phi_{DP}$  than another (Ryzhkov and Zrnich, 1998a) and can give rise to negative  $K_{DP}$ . Gradients along the beam lead to biases in inferred  $K_{DP}$  (Gorgucci et al., 1999a) whereby, for example, a sudden change in  $Z$  of 30dBZ can bias the value of  $K_{DP}$  by up to 30%.

- *Extreme sensitivity to clutter.*

If the random phase of a ground clutter signal is added to a precipitation return which has an amplitude ten times larger, then the resultant signal will have a phase noise of  $5^\circ$ . This will render the value of  $\phi_{DP}$  virtually useless, even though the ground clutter will have a  $Z$  (i.e. an intensity) which is 20dB below (i.e. 1% of) the  $Z$  of the precipitation.

- *Sidelobes.*

$\phi_{DP}$  is much more sensitive to signals from mismatched sidelobes than  $Z_{DR}$ . If the phase of the sidelobe signal is mismatched in  $H$  and  $V$ , then again all we need is sidelobe signal which is 20dB below the precipitation return from the main lobe to introduce a  $5^\circ$  noise in  $\phi_{DP}$ .

- *Differential phase shift on backscatter.*

If the particles or rain or hail are large enough for non-Rayleigh scattering then a differential phase shift on backscatter,  $\delta$ , will be introduced as a transient superposed on the monotonic increase in  $\phi_{DP}$  due to propagation and can lead to apparent negative values of  $K_{DP}$ . For rain, Testud et al. (2000) show that the effect is negligible at S-band, but at C-band  $\delta$  is about  $1^\circ$ ,  $4.5^\circ$ , and  $9.5^\circ$  for  $Z_{DR} = 2\text{dB}$ ,  $3\text{dB}$ , and  $4\text{dB}$ , respectively. Ryzhkov and Zrnich (1996) suggest removing the  $\delta$  transient by 'light' filtering over a distance of 2.4km for heavy rain and 'heavy' filtering over 7.2km for light rain.



The result of the above effects is a noisy trace of  $\phi_{DP}$  not always increasing monotonically with range. Filtering is difficult because the extent of the  $\delta$  region may not be known and it leads to an unacceptable loss of spatial resolution. Ryzhkov and Zrnich (1996) suggest using the modulus of  $K_{DP}$  in Eqn 3 to avoid the problem of negative values, but this does not seem physically justifiable.

## 2.5 LDR - Linear Depolarisation Ratio

LDR is defined as  $10 \log (Z_{VH}/Z_H)$ , where  $Z_{VH}$  is the cross-polar return at horizontal polarisation for a vertically polarised transmission. Only oblate particles falling with their major axis at an angle to the vertical or horizontal direction yield a cross-polar return. LDR is able (Frost et al., 1991; Straka et al., 2000) to identify melting snowflakes associated with the bright band, on occasion it can differentiate ice from rain. Finally, ground clutter has anomalous LDR signals.

Fig. 4a demonstrates that raindrops result in negligible depolarisation because they fall with their major axis aligned in the horizontal; the horizontal field excites a single dipole along the major axis which re-radiates with horizontal polarisation. Contrast this with the oblate non-aligned hydrometeor in Fig. 4b; the incident field excites two dipoles along the major and minor axis, and if the polarisabilities along the two axes are not the same then the resultant induced dipole is no longer parallel to the induced field, and so the re-radiated field has an orthogonal or cross-polar component.

The difference in polarisability is largest for wet oblate particles, so the highest values of LDR of about -15dB are associated with melting snowflakes, because such particles rock and roll as they fall. The LDR of melting hail and dry high density ice crystals is in the range -20 to -26dB. Rain has an LDR generally below -30dB but the observed value is often limited by the antenna isolation. The cross and co-polar signals are essentially uncorrelated, so if the error in  $Z$  is about 0.5dB, then value of LDR can be estimated to 0.7dB. Masking out of echoes where  $LDR > -10$ dB removes much of the ground clutter (see Section 4).

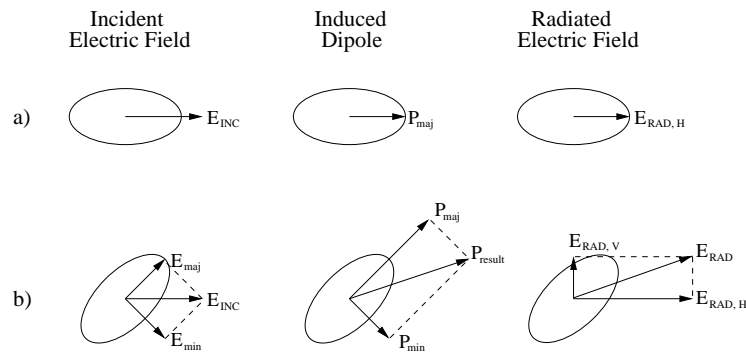


**Fig. 4.** Linear Depolarisation Ratio. a) No depolarisation of incident wave by aligned raindrops. b) Depolarisation by non-aligned oblate spheroids.

## 2.6 An example of a PPI scan through vigorous convection

An S-band low elevation PPI scan through vigorous convective showers which illustrates the signatures of  $Z$ ,  $Z_{DR}$  and  $\phi_{DP}$  is displayed in Fig. 5 which also appears as a colour plate. The observations were made with the Chilbolton  $0.28^\circ$  beamwidth radar in the UK on 28 July 2000 at 1308UT at  $0.5^\circ$  elevation, so that the beam is dwelling in the rain. Because of the narrow beamwidth we believe that this image is not affected by any of the artifacts discussed above such as sidelobes and reflectivity gradients either across or along the main beam. From Fig 5 we see that once  $Z$  is above about 35dBZ then  $Z_{DR}$  reaches about 1dB, but that the high phase shifts generally result from regions of  $Z$  above 45dBZ extending over a few km. Two such regions producing large phase shifts are clearly visible: one at 90km E and -12km N, the other at 115km E and about -8km N. Even for such large phase shifts the estimates of  $K_{DP}$  from differentiating the phase are quite noisy and have a spatial resolution which is much less than the 300m of the  $Z$  and  $Z_{DR}$  and observations. Note that the highest values of  $Z_{DR}$  are about 4dB but are quite localised and often not coincident with the highest  $Z$ ; they do not produce any phase shift and we believe that they result from low concentrations of anomalously large rain drops.

## 3 Raindrop Shapes and Size Spectra

### 3.1 Introduction

Both  $Z_{DR}$  and  $K_{DP}$  essentially provide information on the mean shape and hence the size of raindrops. If this is to lead to improved rainfall rate estimates, then the shape of raindrops as a function of size must be known precisely, but there is currently some uncertainty over these shapes. In addition, if the size sensed by the radar is to be related to the appropriate mean drop size for the rainfall rate then we need to know the range of size spectra for naturally occurring rainfall. Again there is some uncertainty over these spectra.

### 3.2 Raindrop Shape Model

Until very recently, a simple ‘linear’ relationship between axial ratio,  $r$ , and drop diameter,  $D$  in mm, was in widespread use (Pruppacher and Pitter, 1971):

$$r = 1.03 - \beta D \quad (4)$$

with  $\beta$  having a value of  $0.062 \text{ mm}^{-1}$  for drops larger than 0.5mm diameter; drops smaller than 0.5mm are assumed to be spherical. However, in some of the earliest observations Goddard et al. (1982) found that observed values of  $Z_{DR}$  in the range 0dB to 1.5dB were from 0.5 to 0.2dB lower than the values of  $Z_{DR}$  computed using the linear shapes from a raindrop disdrometer at the ground 200m below the radar beam. They could only obtain agreement if they empirically adjusted the shape of drops smaller than 2.5mm to be more spherical

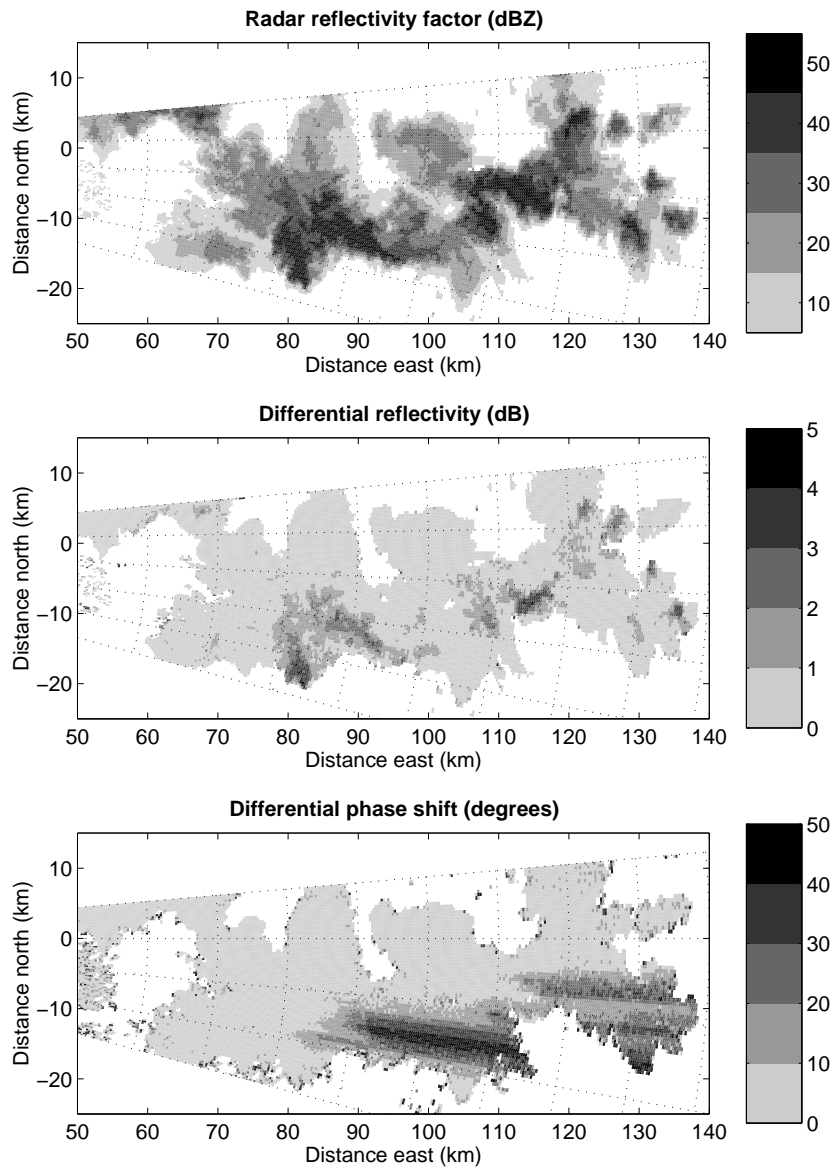


**Fig. 5.** An example of  $Z$ ,  $Z_{DR}$  and  $\phi_{DP}$  observed with the narrow beam S-band Chilbolton radar in the UK on 28 July 2000. The data are from a low elevation ( $0.5^\circ$ ) PPI scan, so the beam is dwelling in the rain. Even for these large values of  $\phi_{DP}$  the derived values of  $K_{DP}$  are rather noisy with much poorer range resolution than  $Z$  and  $Z_{DR}$ . Figure courtesy of R.J.Hogan (U of Reading). Radar data kindly supplied by RCRU, Rutherford Appleton Laboratory.

than given by Eqn 4. They proposed (Goddard et al., 1995) a new drop shape model:

$$r = 1.075 - 0.065D - 0.0036D^2 + 0.0004D^3 \quad (5)$$

for drops larger than 1.1mm with smaller drops again assumed spherical. Confirmation of such drop shapes is not simple. If the raindrop shape is measured close to the ground then the drops have just experienced atypically high shear as they fall through the boundary layer. Similarly, drop shapes measured with in-situ aircraft probes have been subjected to unusual stresses as they are deflected around the aircraft wing. It is only recently that careful experiments in long wind tunnels such as those carried out by Andsager et al. (1999), and references therein, have proposed the following polynomial:

$$r = 1.012 - 0.01445D - 0.01028D^2 \quad (6)$$

for  $D$  in the range 1-4mm. The three drop shape models are compared in Fig. 6. Eqns 5 and 6 are very similar and predict virtually the same values of  $K_{DP}$  and  $Z_{DR}$ . This remarkable independent confirmation of the empirical adjustment gives us confidence that the ‘linear’ shapes are indeed an oversimplification and that these ‘new’ drop shapes are probably correct. The last two Eqns lead to negligible differences in the predicted polarisation parameters; when we refer to ‘new’ drop shapes we will be using those of Eqn 5 as opposed to the ‘linear’ shapes of Eqn 4. Eqn 6 is equally valid.

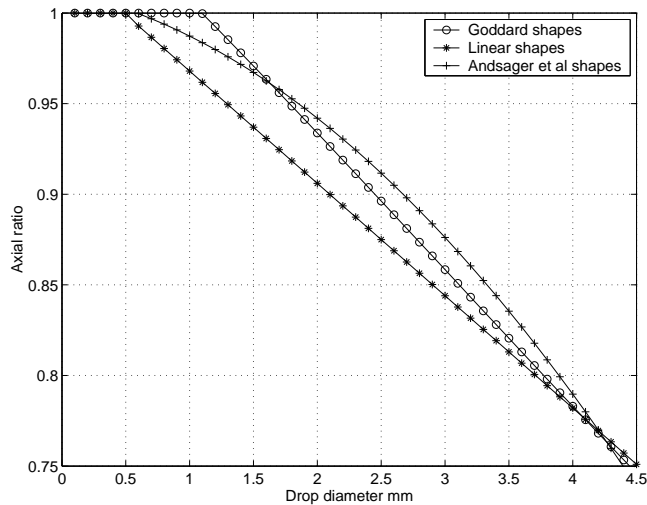


**Fig. 6.** Different raindrop shapes models.

The linear drop shapes used in the past lead to two effects. Firstly, the linear drop shapes are more oblate than those occurring naturally leading to predicted

values of  $Z_{DR}$  and  $K_{DP}$  which are too high so that values of ‘ $c$ ’ in Eqn 2 and ‘ $a$ ’ in Eqn 3 are too small; this may account for the underestimates of rainfall using  $K_{DP}$  reported, for example, by May et al. (1999) and Petersen et al. (1999) who used the ‘linear’ raindrop as discussed by Bringi and Chandrasekar (2001). Secondly, for drops in the range 1-3mm the ‘new’ drop shapes predict a larger value of  $\beta$  than the 0.062 in Eqn 4; this means that the increase in the values of  $Z_{DR}$  and  $K_{DP}$  as the rainfall rate increases will be more rapid than predicted from the linear drops, so that in reality the value of ‘ $b$ ’ in the  $R(K_{DP})$  exponent will be lower than the value of 0.866 predicted using linear shapes (Illingworth and Blackman, 2002).

### 3.3 Raindrop Size Spectra

To gauge the performance of polarisation techniques in improving rainfall estimates we need to know how variations in the drop size spectra affect the representativeness of the mean drop size inferred from the polarisation parameters. Rather than the simple exponential representation in Eqn 1, natural raindrop size spectra are well represented by a normalised gamma function of the form

$$N(D) = N_w f(\mu) \left( \frac{D}{D_0} \right)^\mu \exp \left( -\frac{(3.67 + \mu)D}{D_0} \right) \quad (7)$$

where

$$f(\mu) = \frac{6}{(3.67)^4} \frac{(3.67 + \mu)^{\mu+4}}{\Gamma(\mu + 4)} \quad (8)$$

which when  $\mu = 0$  reduces to the simple exponential form of Eqn 1 with  $N_w \equiv N_0$ . This form has the advantage that the three variables are independent, with  $D_0$  being the median volume drop diameter,  $\mu$  being the shape of the drop spectrum, and  $N_w$  is a normalised drop concentration so that the liquid water content remains constant even if  $\mu$  changes, and is preferable (Illingworth and Blackman, 2002) to the non-normalised gamma function of Ulbrich (1983),

$$N(D) = N_0 D_0^\mu \exp \left( -\frac{(3.67 + \mu)D}{D_0} \right) \quad (9)$$

We have followed the convention of Bringi and Chandrasekar (2001);  $N_w$  is the same as the  $N_L$  used by Illingworth and Blackman (1999, 2002) and the  $N_0^*$  used by Testud et al. (2001, 2003 - this book), with ‘w’ and ‘L’ both indicating normalisation with respect to liquid water content. These equations are sometimes expressed in terms of  $D_m$ , the mass weighted mean diameter, in which case  $D_m$  is equal to  $D_0$  times the factor  $(4 + \mu)/(3.67 + \mu)$ .

Ulbrich (1983) derived the expected range of values of  $N_0$  and  $\mu$  in the non-normalised Eqn 9 in natural rainfall by comparing expressions for  $R$  and  $Z$  from the appropriately weighted integral of Eqn 9 with the 69  $Z(R)$  relationships of Battan (1973); he deduced the range of  $\mu$  was from -1 to 5. The mathematical validity of this approach for deriving the ‘Ulbrich’ range of values of  $N_0$  and  $\mu$  has

been questioned by Illingworth and Blackman (2002), but it has become common practice to derive relationships between  $R$  and the polarimetric variables by cycling over these ‘Ulbrich’ values of  $N_0$  and  $\mu$ , calculating  $Z$ ,  $Z_{DR}$ ,  $K_{DP}$  and  $R$  and performing a non-linear regression.

We now explore other methods of deriving the range of values of  $\mu$ ,  $N_w$  and  $D_0$  in naturally occurring rainfall. One approach is to use observed raindrop spectra. A least squares fit is not appropriate because it gives equal weight to small and large rain drops, whereas for radar and rainfall the larger drops are much more important. Kozu and Nakamura (1991) and Illingworth and Johnson (1999) both equated the sixth, fourth and third moments of observed raindrop size distributions to the appropriately weighted integral of the gamma function and deduced values of  $\mu$  in the range 0 to 15 with a mean value of about 5 or 6. Illingworth and Johnson (1999) found that in the UK the mean value of the normalised raindrop concentration,  $N_w$ , was close to the Marshall-Palmer value of  $8000 \text{ m}^{-3} \text{ mm}^{-1}$  with a standard deviation of a factor of three. Bringi and Chandrasekar (2001) found a similar spread of  $N_w$  when they analysed an entire season of rainfall spectra from Darwin, Australia.

These high values of  $\mu$  derived from fitting the higher moments have been criticised because they are very dependent upon maximum drop size in the spectra which are poorly sampled by disdrometers. The values obtained depend upon the moments chosen for the fit. Higher moments are appropriate for relationships between  $Z$  and  $R$  and lead to higher values of  $\mu$ . Testud et al. (2001) and Bringi and Chandrasekar (2001) infer  $\mu$  values closer to unity; this may be because they first derive  $N_0$  and  $D_0$  in an exponential spectrum by fitting moments, but then choose  $\mu$  to minimise a least squares fit to the observed spectrum. This procedure for fixing  $\mu$  assigns equal weight to drops of all sizes and may lead to values of  $\mu$  which are inappropriate for the higher moments involved in radars studies. Ulbrich and Atlas (1998) used truncated moments by limiting the experimental spectra to  $D_{max}$  and found that this reduced  $\mu$  from about 4 to a median value of 0 with a mean of 1.6.

The disadvantage with the above techniques is the use of a disdrometer which has poor sampling of the larger drops which are important for the higher moments. This can be avoided by appealing to radar measurements themselves; because of the much larger radar sampling volume the large drops are sampled satisfactorily. Wilson et al. (1997) reported values of  $\mu$  derived from the ‘Differential Doppler Velocity’, DDV, the difference in the Doppler velocity of rain for horizontally and vertically polarised radiation with the radar beam dwelling at a finite elevation. They showed that the value of DDV as a function of  $Z_{DR}$  depends upon the value of  $\mu$  and found a range of  $\mu$  between 2 and 10 with a mean value of 5. There is also some evidence from observations of the Doppler spectral width of rainfall at vertical incidence which indicate (pers. comm., D. Bouniol) that the width is significantly narrower than would be observed for an exponential and is consistent with a  $\mu$  of around 5.

### 3.4 Implications for $Z = aR^b$ Relationships

It appears that the range of naturally occurring raindrop size spectra is accurately described by the normalised gamma function in Eqn 7 with values of  $\mu$  near 5 and values of  $N_w$  which have a standard deviation of factor of three. We now follow the treatment of Bringi and Chandrasekar (2001) and show that the normalised gamma function leads to  $Z(R)$  relationships of the form  $Z = aR^{1.5}$  with different values of 'a' reflecting changes in  $N_w$ . There is however an additional dependence of 'a' upon the value of  $\mu$ . Integrating the appropriately weighted normalised gamma function produces expressions of the form:

$$Z = F_Z(\mu)N_w D_0^7, \quad (10)$$

and assuming the terminal velocity varies as  $D^{0.67}$ ,

$$R = F_R(\mu)N_w D_0^{4.67}; \quad (11)$$

eliminating  $D_0$  gives

$$\frac{Z}{N_w} = H(\mu) \left( \frac{R}{N_w} \right)^b \quad (12)$$

where  $b = 7/4.67 \approx 1.5$  or:

$$Z = H(\mu)N_w^{1-b} R^b = \frac{H(\mu)R^{1.5}}{\sqrt{N_w}}. \quad (13)$$

It is usually assumed that  $H(\mu)$  is a slowly varying function of  $\mu$ . This is so if we restrict  $\mu$  to the range 0 to 2, but earlier we argued that  $\mu$  has an average value of 5, and can vary between 0 and 10. As  $\mu$  increases from 0 to 5 and 10, the value of  $H(\mu)$  falls by a factor of 1.55 (2dB) and 1.79 (2.5dB).

Accordingly we can associate changes in the multiplicative factor 'a' in  $Z = aR^b$  not only with changes in  $N_w$  but also with  $\mu$ . For example, a standard deviation of  $N_w$  of a factor of three will lead to a change in 'a' of a factor of 1.7, and a change in rainfall rate derived from  $Z$  of  $\pm 40\%$ . To this we must add a similar change in 'a' and  $Z$  from the range of  $\mu$ ; if the two are uncorrelated then the error in  $R$  will be about 64%. If the range of values of  $N_w$  is a factor of ten: this will lead to changes in 'a' of a factor of three, and a factor of two error in the rain rate. This gives us a good estimate of the error expected by a simple  $Z = aR^b$  relationship because of variability in drop spectra. In Section 6 we will discuss a simple polarimetric method of estimating  $N_w$  and hence gauging the value of 'a', leaving only the variability due to the unknown  $\mu$ .

## 4 Identification of Ground Clutter and Anomalous Propagation

Anomalous Propagation can be one of the most difficult signals to reject using conventional radar (e.g. Pamment and Conway, 1998) but fortunately their identification via polarisation returns is unambiguous. Both clutter and 'anaprop'

give rise to non-Rayleigh scattering so that the both the amplitudes and phases of the H and V returns are essentially uncorrelated. Accordingly, these signals can be identified by:

- The most reliable technique relies upon a copolar correlation of essentially zero as opposed to values above 0.9 for precipitation echoes (Caylor and Illingworth, 1992; Ryzhkov and Zrnic, 1998b).
- A noisy  $\phi_{DP}$  profile (Ryzhkov and Zrnic, 1998b)
- Higher values of LDR than occur in natural precipitation (Wilson et al., 1995; Hagen, 1997).
- Noisy estimates of  $Z_{DR}$  which fluctuate between  $\pm 3$ dB from gate to gate (Hall et al., 1984).

## 5 Improved Rainfall Rates using Polarisation Parameters

### 5.1 Introduction

In this section we discuss the improved accuracy in rainfall rates by using  $Z_{DR}$  or  $K_{DP}$ . The error in  $R$  derived from  $Z$  alone can be up to a factor of two; the goal is to reduce this to  $\pm 25\%$ . We shall initially consider cases when we know that the beam is dwelling in rain and there is no ice present. This will apply to summer time situations in the mid-latitudes out to a range of about 75km when the melting layer is above 2km and no hail is present. The situation is more common in the tropics because the melting level is much higher and large hail is rarer.

### 5.2 $R = f(Z, Z_{DR})$

The procedure outlined in Section 2.2 for calculating rainfall from  $Z$  and  $Z_{DR}$  seems straightforward. Bringi and Chandrasekar (2001) suggest that at S-band  $D_0 = 1.529Z_{DR}^{0.467}$  (with  $Z_{DR}$  in dB) and that we should be able to estimate  $D_0$  from  $Z_{DR}$  to within 0.1mm, but plots of  $D_0$  as a function of  $Z_{DR}$  computed for normalised gamma functions (Fig. 7) with the ‘new’ drop shapes are initially discouraging, showing great sensitivity to  $\mu$ . From Fig. 7, if  $Z_{DR} = 1.5$ dB and  $\mu = 0$  then we have  $D_0 = 1.5$ mm but for the narrower spectrum with  $\mu = 5$  and the same  $Z_{DR}$ , the absence of larger drops in the tail of the spectrum means that we need  $D_0 = 2.2$ mm. However, the goal is to measure  $R$  not  $D_0$ , and  $R$  is a function of both  $D_0$  and  $\mu$ . Fortunately, for  $D_0 = 2.2$ mm and  $\mu = 5$ , both the rainfall rate and the value of  $Z$  are about five times higher than for  $D_0 = 1.5$ mm and  $\mu = 0$ . As we shall see in the next paragraph, this means that the value of  $Z$  per unit  $R$  as a function of  $Z_{DR}$  for the normalised gamma functions has a much reduced dependence upon  $\mu$ , with the curves for  $\mu = 0$  and  $\mu = 5$  only 1dB apart.

In Section 2.2 we argued that  $Z/R$  should be a function of  $Z_{DR}$  (Eqn 2). Values of  $Z/R$  as a function of  $Z_{DR}$  for the ‘linear’ (Eqn 4) and ‘new’ (Eqn 5) drop shapes are plotted in Fig. 8. These curves can be interpreted as the  $Z$



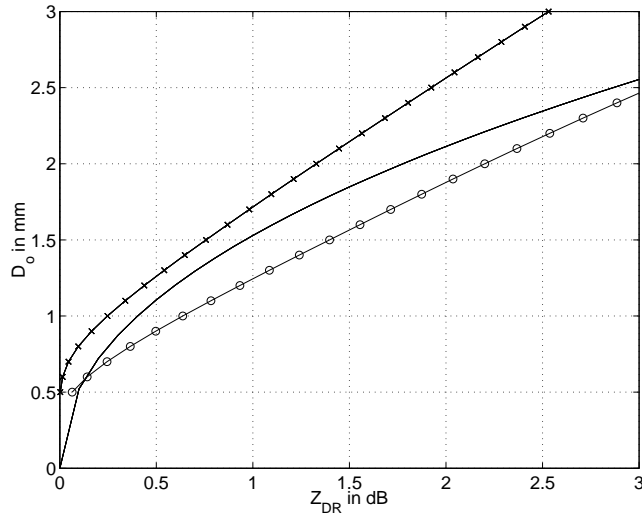


**Fig. 7.** Plot of  $D_0$  against  $Z_{DR}$  for the new drop shape models at S-band with  $\mu = 0$  (o) and  $\mu = 5$  (x). The solid line is  $D_0 = 1.529Z_{DR}^{0.467}$  suggested by Bringi and Chandrasekar (2001)

which would give  $R$  of  $1 \text{ mm hr}^{-1}$  for a particular value of  $Z_{DR}$ . The rain rate scales with  $Z$ , so, if for a given  $Z_{DR}$ , the observed value of  $Z$  is ' $x$ ' dB above the line then the rain rate is ' $x$ ' dB above  $1 \text{ mm hr}^{-1}$ .

It was argued in Section 3.3 that  $\mu$  of 5 is the average value for natural rainfall. A third order polynomial fit of  $Z/R$  as a function of  $Z_{DR}$  for  $\mu = 5$ , gives the following expression for Eqn 2 (Illingworth and Blackman, 2002) :

$$Z/R = 21.48 + 8.14Z_{DR} - 1.385(Z_{DR})^2 + 0.1039(Z_{DR})^3 \quad (14)$$

at S-band which is accurate to 0.5dB. The equivalent expression at C-band is:

$$Z/R = 21.50 + 8.35Z_{DR} - 1.89(Z_{DR})^2 + 0.1976(Z_{DR})^3 \quad (15)$$

This assumes that the values of  $Z_{DR}$  have been corrected for any attenuation to an accuracy of 0.2dB.

An alternative approach has been widely adopted in the literature (see discussion in Bringi and Chandrasekar (2001)) in which the requirement for  $Z$  to scale with  $R$  for constant  $Z_{DR}$  is dropped and a relationship of the form

$$R = c_1 Z_H^{a_1} 10^{0.1b_1 Z_{DR}} \quad (16)$$

is used. The coefficients are chosen by allowing the  $N_w$  (or  $N_0$ ),  $D_0$  and  $\mu$  to cycle over the 'Ulbrich' (Secn 3.3) range of values, calculating  $Z$ ,  $Z_{DR}$  and  $R$  and performing a non-linear regression. The curve proposed by Bringi and

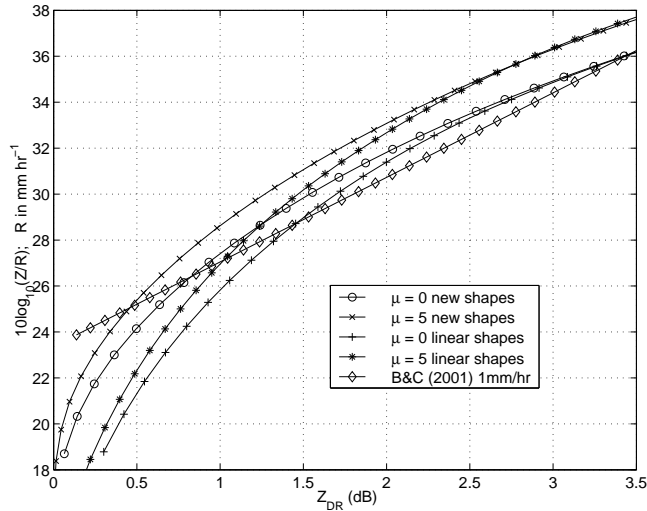


Fig. 8. Plot of  $Z/R$  against  $Z_{DR}$  for the linear and new drop shape models at S-band

Chandrasekar (2001) with  $c_1 = 0.0067$ ,  $a_1 = 0.93$ ,  $b_1 = -3.43$  at S-band using the ‘new’ drop shapes for  $R = 1 \text{ mm hr}^{-1}$  is also plotted in Fig.8 and predicts rainfall rates 2dB higher than Eqn 14 once  $Z_{DR}$  is above 1dB. For a higher rain rate of  $10 \text{ mm hr}^{-1}$  the non-linearity with  $Z$  introduced by  $a_1 = 0.93$  means that the curve would be 0.7dB higher, but the rainfall overestimate would be still over 1dB. Physically, it is difficult to justify using a value of  $a_1$  which is not unity, unless the heavier rainfalls are systematically associated with higher values of  $\mu$ . Earlier relationships based on Eqn 16 (Gorgucci et al., 1994; Chandrasekar and Bringi, 1988; Chandrasekar et al., 1990) used the linear drop shapes and the ‘Ulbrich’ range of  $N_0$  and  $\mu$  (Illingworth and Blackman, 2002) leading to curves about 1-2dB lower than the values of Bringi and Chandrasekar (2001) and a probable overestimate of the rainfall rate by up to a factor of two.

If we seek a value of  $R$  accurate to  $\pm 25\%$  (1dB) then from Fig. 8 we note:

- *Accuracy of  $Z_{DR}$  estimate*  
A 25% accuracy in  $R$  implies that  $Z/R$  should be known to 1dB, which from the slope of the curves imposes a limit of 0.2dB for the accuracy of the  $Z_{DR}$  estimate for  $R > 10 \text{ mm hr}^{-1}$ . For a rainfall rate of  $3 \text{ mm hr}^{-1}$  an accuracy of 0.1dB is needed. As we saw in Section 2.2 this is very difficult to achieve.
- *Calibration of  $Z$*   
 $R$  is only as accurate as the value of  $Z$ , so a 25% error in  $R$  implies that  $Z$  must be calibrated to 1dB. This is a serious constraint and will be discussed further in Section 6.
- *Sensitivity to drop shapes*  
The correct choice of drop shapes is crucial. The ‘new’ drop shapes will lead to rainfall rates from 1 or 3dB lower than the traditional ‘linear’ shapes.

Using the Andsager shapes (Eqn 6) rather than Goddard shapes (Eqn 5) changes the values of  $Z/R$  by less than 0.5dB.

- *Theoretical limit to accuracy of  $R$  estimate*  
Supposing that the drop shapes are known, then the naturally occurring variability of  $\mu$  limits the fundamental accuracy of the technique. If the mean value of  $\mu$  in rain is 5, but varies between 2 and 10, then this will introduce an uncertainty in the  $R$  estimates of about 0.5dB or  $\pm 12\%$ . A greater variability of  $\mu$  with values down to 0 implies an error of 1dB or 25%.
- *Sensitivity to truncation of drop spectrum*  
A value of  $\mu = 5$  in rain introduces a natural truncation of the drop spectrum so that the curves in Fig. 8 are insensitive to the choice of maximum drop size providing it is larger than 8mm.

### 5.3 $R = f(K_{DP})$

The potential advantages of deriving  $R$  from  $K_{DP}$  were summarised in Section 2.4 tempered by remarks on the noisy character of observed values of  $K_{DP}$ . Plots of the values of  $K_{DP}$  (one-way) as a function of  $R$  at S-band for the ‘linear’ and ‘new’ drop shape models using the normalised gamma function with  $\mu = 0$  and 5 with constant  $N_w = 8000 \text{ m}^{-3} \text{ mm}^{-1}$  are displayed in Fig.9 and demonstrate:

- *Sensitivity to drop shape model.*  
For a value of  $K_{DP}$  of  $0.55^\circ \text{ km}^{-1}$ , the linear drop shapes with  $\mu = 0$  predict a rainfall of about  $20 \text{ mm hr}^{-1}$  rather than about 25 and  $30 \text{ mm hr}^{-1}$  for the ‘new’ drop shapes with  $\mu = 0$  and 5, respectively. This may account for the persistent underestimates of rainfall using  $K_{DP}$  with these drop shapes (e.g. most recently, Brandes et al. (2001)) from the widespread use of the Eqn:

$$R = 40.56K_{DP}^{0.866} \quad (17)$$

Bringi and Chandrasekar (2001) suggest using a coefficient of 50.7 rather than 40.56 is more appropriate for the ‘new’ drop shapes.

- *Increased non linearity and sensitivity to drop concentration and  $\mu$*   
We have argued that  $\mu = 5$  is more appropriate than  $\mu = 0$ ; over the range 10-100  $\text{mm hr}^{-1}$  with the new drop shapes at S-band (9.75cm) this yields:

$$R = 50.1K_{DP}^{0.7} \quad \text{or} \quad K_{DP} = 0.00417R^{1.4} \quad (18)$$

Note that the index for  $R$  of 1.4 in Eqn 18 is almost as large as the value of 1.5 derived for a  $Z(R)$  relationship in Section 3.4 and identical to the index for the NEXRAD default  $Z(R)$  relationship ( $Z = 300R^{1.4}$ ) quoted in Brandes et al. (1999). This suggests that apart from the immunity to hail, many of the advantages claimed for the  $R(K_{DP})$  approach may be difficult to realise. Increases of  $N_w$  of a factor of ten will lead to the inferred rainfall rate being underestimated by a factor of two for all values of  $R$ . Changing  $\mu$  from 5 to 0 reduces  $R$  by about 30% for values of  $R$  of about  $20 \text{ mm hr}^{-1}$ .

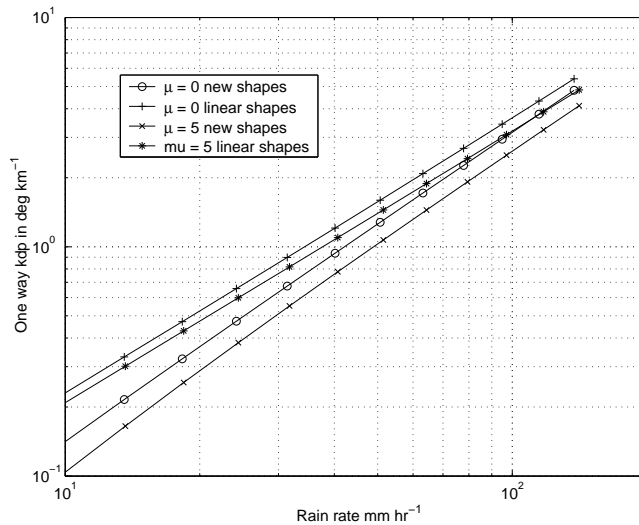


**Fig. 9.** Plot of  $R$  against one-way  $K_{DP}$  at S-band for the linear and new drop shape models with  $N_w = 8000 \text{ m}^{-3} \text{ mm}^{-1}$  and  $\mu = 0$  and 5.

The  $R(K_{DP})$  dependence at C-band is similar to that shown in Fig.9 but with the values of  $K_{DP}$  approximately scaled by the increased frequency. The appropriate equation for the ‘new’ drop shapes and  $\mu = 5$  at C-band (5.35cm) is:

$$R = 31.4K_{DP}^{0.7} \quad \text{or} \quad K_{DP} = 0.00802R^{1.4} \quad (19)$$

Matrosov et al. (1999) present differential phase observations at X-band (3.2cm) and suggest an equation similar to Eqn 19 for rain rates up to  $15 \text{ mm hr}^{-1}$  with a coefficient of 14.2 and an exponent of 0.85 for the linear shapes in Eqn 4 with  $\beta$  of  $0.062 \text{ mm}^{-1}$ , but found better agreement with rain gauges if they used much less oblate drops with a rather unrealistic  $\beta$  of  $0.044 \text{ mm}^{-1}$  which gave a coefficient of 20.5. For these rain rates they calculated that the maximum value of  $\delta$  was an insignificant  $1^\circ$ . Although  $\phi_{DP}$  is larger at X-band, in heavy rain the bigger drops will Mie scatter, so  $\delta$  will be larger and the correlation lower; both effects lead to an increasingly noisy  $\phi_{DP}$ .

Thus far we have only discussed the form of the  $R(K_{DP})$  dependence. The next stage is to consider the error in the derived values of  $R$ ,  $\sigma_R$ , resulting from the error in the differential phase estimate  $\sigma_\phi$  which can in theory be as low as  $1^\circ$  but in practice is at least  $3^\circ$ . The value of the one-way  $K_{DP}$  is derived by a least squares fit through the  $N$  gates each of length  $\Delta(r)$  to give a range resolution of  $L = N\Delta(r)$  and has an error given by:

$$\sigma_{K_{DP}} = \frac{\sigma_\phi}{L} \sqrt{\frac{3}{N - (1/N)}} \quad (20)$$

The errors in  $K_{DP}$  predicted from this Eqn appear quite encouraging (Bringi and Chandrasekar, 2001); with a gate length of 150m, a resolution of 2.4km, and  $\sigma_\phi$  of 1 and 3° the value of  $\sigma_{K_{DP}}$  from a fit over the 16 gates is 0.18 and 0.54° km<sup>-1</sup>, respectively. However, Blackman and Illingworth (1997) extended the analysis to the context of an operational radar and derived the error in the rainfall rate,  $\sigma_R$ , with an azimuthal resolution  $L$  to match the range resolution, for a radar with a beamwidth of  $\theta_b$  at a range  $r$ , and derived an expression:

$$\sigma_R = \frac{\sigma_\phi}{abR^{b-1}L^2} \sqrt{12\theta_b r \Delta(r)} \quad (21)$$

where  $\theta_b$  is in radians,  $R$  is the rainfall rate and  $a$  and  $b$  are the constants in the expression  $K_{DP} = aR^b$ . This leads to the following errors in rainrate estimates:

- *Resolution of 2.4km, range of 25km, and  $\sigma_\phi$  of 1°*  
An  $R$  of 10mm hr<sup>-1</sup> can be estimated to 60% and  $R=50$ mm hr<sup>-1</sup> to 6%.
- *For a more realistic  $\sigma_\phi = 3^\circ$  and range = 100km*  
The accuracy for  $R = 10$  and 50 mm hr<sup>-1</sup> is 361% and 40%.
- *Performance at C-band*  
At C-band the value of  $b$  is about half that at S-band, so these percentages would be reduced by a factor of two, provided low values of  $\sigma_\phi$  can be achieved at C-band.
- *Performance at 4.8km resolution rather than 2.4km*  
The fractional errors are reduced by a factor of four, but at a range of 100km the S-band error at 10 mm hr<sup>-1</sup> would be still 90% and 10% for 50mm hr<sup>-1</sup>.

The remaining possibility is to multiply the dwell time by four which would halve the phase error,  $\sigma_\phi$  and the rain rate error,  $\sigma_R$ , but lead to an unacceptably slow scanning rate. The use of the integrated differential phase shift,  $\Phi_{DP}$ , along a path length of 30km (Ryzhkov et al., 2000) and 10km (Bringi et al., 2001a) and exploiting the assumed linearity of the  $R(K_{DP})$  relationship to provide an integrated average rainfall over a catchment has been proposed but, for most applications, this approach leads to an unacceptable loss of spatial resolution. We are forced to conclude that the noisy characteristics of  $\phi_{DP}$  mean that  $K_{DP}$  cannot provide sufficiently accurate rainfall rates at the scales of 2km required in an operational environment.

## 6 Improved Rainfall Rate Using Integrated Polarisation Parameters

In this section we analyse what information can be retrieved from the three parameters  $Z$ ,  $Z_{DR}$  and  $K_{DP}$ . First we look at their use in an operational environment and conclude that their accuracy is probably insufficient to provide an improved rainfall rate using all three parameters on the 2km scale, but that their integrated properties can provide a valuable constraint. We then consider how the non-independence of the three parameters can be used to provide an auto-calibration of  $Z$  to within 0.5dB every time there is heavy rain. Next we

discuss an alternative approach whereby the radar is assumed calibrated but the non-independence of the parameters is used to derive a drop shape model. Finally we consider the ‘ZPHI’ technique, whereby the value of the integrated phase shift is used to fix the value of ‘a’ in the  $Z = aR^b$  relationship.

### 6.1 R from Z, $Z_{DR}$ and $K_{DP}$

In the previous section deriving  $R$  from  $Z$  and  $Z_{DR}$  or from  $K_{DP}$  were discussed. A natural progression would seem to be to use all three parameters,  $Z$ ,  $Z_{DR}$  and  $K_{DP}$  from which one might derive the three parameters of the normalised gamma function,  $N_w$ ,  $D_0$  and  $\mu$  and hence an improved rainfall rate. Several authors have published equations of the form:

$$R(K_{DP}, Z_{DR}) = cK_{DP}^a Z_{DR}^b \quad (22)$$

with the values of  $a$ ,  $b$ , and  $c$  obtained by a regression analysis of values obtained by scanning over the ‘Ulbrich’ values of  $N_0$ ,  $D_0$  and  $\mu$ . Bringi and Chandrasekar (2001) provide a table of the coefficients in Eqn 22 with, for example, at S-band  $c = 90.8$ ,  $a = 0.89$  and  $b = -1.69$  (for  $Z_{DR}$  in linear units). Four comments may be made concerning this approach:

- *Physical arguments would lead us to expect that  $a = 1$*   
For a given value of  $Z_{DR}$ , both  $R$  and  $K_{DP}$  should scale linearly with  $N_w$ .
- *The Z information is not used at all*  
 $Z$  can be estimated more accurately than either  $Z_{DR}$  or  $K_{DP}$ , but of course  $Z$  must be calibrated whereas  $Z_{DR}$  and  $K_{DP}$  are ‘self-calibrating’.
- *Insensitivity to hail*  
Although  $K_{DP}$  is very noisy, it has the unique advantage that it is insensitive to hail, but in the above equation this advantage is lost. Hail will lead to a reduced value of  $Z_{DR}$  and an erroneous inferred rainfall rate.
- *Non-independence of Z,  $K_{DP}$  and  $Z_{DR}$  in rainfall*  
Once  $Z$  and  $Z_{DR}$  are known then the value of  $K_{DP}$  can be derived.

### 6.2 Auto-calibration of Z using Polarisation Redundancy.

Calibration of  $Z$  is sometimes neglected but is crucial if accurate rainfall rates are to be derived from  $Z$  alone or from both  $Z$  and  $Z_{DR}$ . Traditional methods rely on characterising the link-budget or comparisons with rain gauges but are often only good to a factor of two. Goddard et al. (1994) showed (Fig 10) that for rain  $K_{DP}/Z_H$  is a unique function of  $Z_{DR}$  which is virtually independent of  $\mu$  and proposed that this redundancy could be used to provide an automatic calibration of  $Z$  to within 0.5dB each time there was moderately heavy rainfall. The technique is as follows: The observed value of  $Z$  and  $Z_{DR}$  at each gate along a ray are used to predict the value of  $K_{DP}$  at that gate and so the predicted phase shift at each gate can be calculated and added up to give the theoretical total phase shift along the ray,  $\Phi_{DP}$ . This total phase shift can be compared

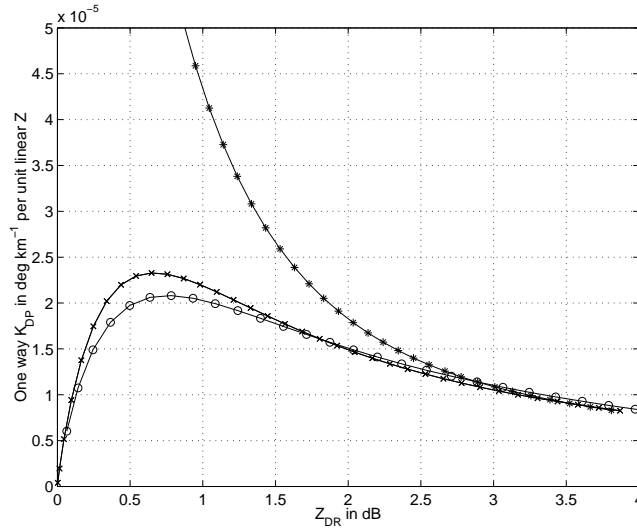


**Fig. 10.** Autocalibration technique for  $Z$  at S-band. Values of one-way  $K_{DP}/Z$  for the normalised gamma function as a function of  $Z_{DR}$ . ‘New’ shapes: ‘o’  $\mu = 0$ ; ‘x’,  $\mu = 5$ . ‘Linear’ shapes: ‘\*’  $\mu = 5$ .

with the observed total phase shift and the value of  $Z$  scaled until the computed value agrees with the observed value as illustrated in Fig. 11. The technique has the following advantages:

- *The total phase shift is a robust observation*  
The technique avoids deriving  $K_{DP}$  by differentiating an observed noisy  $\phi_{DP}$  profile to give an even noisier gradient, but instead uses the two almost constant values of  $\phi_{DP}$  before and after the heavy rain..
- *Calibration accuracy of 10% or 0.5dB*  
This can be achieved if an observed  $\Phi_{DP}$  of  $10^\circ$  can be estimated to  $1^\circ$  accuracy. The calibration can be repeated for many rays so that any anomalous rays with very noisy  $Z_{DR}$  or  $\phi_{DP}$  can be recognised and rejected.
- *Insensitivity to errors in  $Z_{DR}$*   
Most of the phase shift occurs with  $Z_{DR}$  of between 1 and 2dB, so from the slope of the curve in Fig 10 we only need estimate  $Z_{DR}$  to about 0.4dB to achieve the required calibration accuracy of 0.5dB.
- *The drop shape model provides a limit to the attainable accuracy*  
The use of the ‘linear’ drop shapes rather than the new ones changes the calibration typically by about 1dB (see Fig 10).
- *The effect of attenuation*  
Le Bouar et al. (2001) express concern over attenuation of  $Z$  and  $Z_{DR}$ . The technique does indeed fail at X-band, but if  $\Phi_{DP}$  at C-band is limited to  $10^\circ$ , then the  $Z$  attenuation is less than 0.5dB and does not pose a problem.

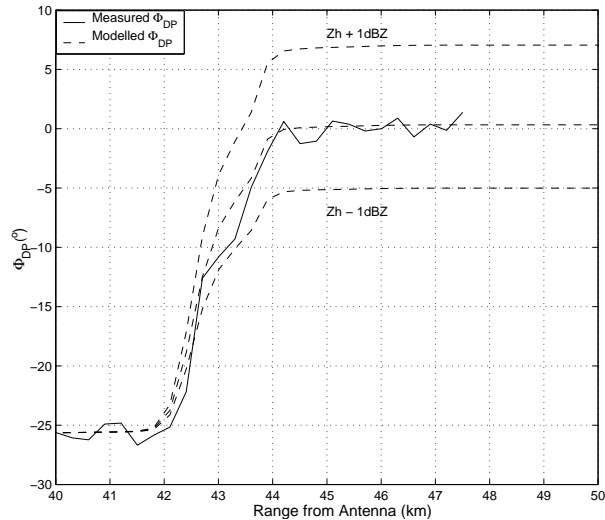


**Fig. 11.** Example of autocalibration. Different calibrations of  $Z$  lead to three different traces for  $\Phi_{DP}$ . Comparison with the observed  $\Phi_{DP}$  in rain fixes the calibration of  $Z$  to 0.5dB (10%). The initial value of  $\phi_{DP}$  is an arbitrary system offset.

Gorgucci et al. (1999b) propose a rather similar calibration technique based upon examination of the consistency between the two polarimetric rain-rate estimates, one using  $Z$  and  $Z_{DR}$  the other using  $K_{DP}$ . Because this method involves deriving  $K_{DP}$  directly from the observations, the noisy value of  $K_{DP}$  introduces considerable scatter into the data, making the comparison rather difficult.

### 6.3 Use of Polarisation Redundancy to Derive Drop Shape Model

A rather different approach in exploiting the non-independence of the polarisation variables in rainfall is to assume that the radar is independently calibrated but allow the raindrop shape versus size relationship to be a free variable which is fixed by the observations. Gorgucci et al. (2000) consider the raindrop spectrum to be described as a gamma function and calculate values of  $Z$ ,  $Z_{DR}$ , and  $K_{DP}$  by cycling randomly over the ‘Ulbrich’ (Secn 3.3) range of  $N_0$ ,  $D_0$  and  $\mu$  to be expected and also allow a variation of the values of the slope,  $\beta$ , in Eqn 4 for the linear model of drop shape. A non-linear regression analysis yields:

$$\beta = 2.37 Z_H^{-0.377} K_{DP}^{0.396} 10^{0.093Z_{DR}} \quad (23)$$

They suggest the  $\beta$  can be estimated to 10%. Inferred values in one storm range from 0.04 to 0.08, with average values falling from 0.061 to 0.053 for the  $Z$  ranges 40-45dBZ to above 53dBZ which they ascribe to raindrop oscillations. Gorgucci et al. (2001) use this approach and report rainfall estimates which are immune



to changes in the raindrop shape-size relation. Recently, Matrosov et al. (2002) report that at X-band the use of a variable  $\beta$  leads to improved rainfall rates than from  $K_{DP}$  alone. The immunity to drop shape models provided by this approach is attractive, but the following caveats apply:

- *Apparent change of  $\beta$  with rainfall rate.*

Eqn 23 is virtually identical to the Goddard et al. (1994) calibration curve; the indices of  $Z_H$  and  $K_{DP}$  are nearly equal and opposite, so for a given  $\beta$  the Eqn reduces to a single curve of  $Z_H/K_{DP}$  against  $Z_{DR}$ . Rather than use a non-linear regression, the values of  $Z_H$ ,  $K_{DP}$  and  $Z_{DR}$  as  $D_0$  varies have been calculated for a normalised gamma function with  $\mu = 5$ , and the apparent value of  $\beta$  in Eqn 23 plotted out in Fig. 12 as a function of  $Z_{DR}$  for the ‘new’ drop shapes. From Fig. 12 we now see that the apparent fall of  $\beta$  in heavy (high  $Z_{DR}$ ) rain arises naturally from the fall in the  $K_{DP}/Z$  ratio with increasing  $Z_{DR}$  in the calibration curve Fig. 10, rather than appealing to drop oscillations (Gorgucci et al., 2000).

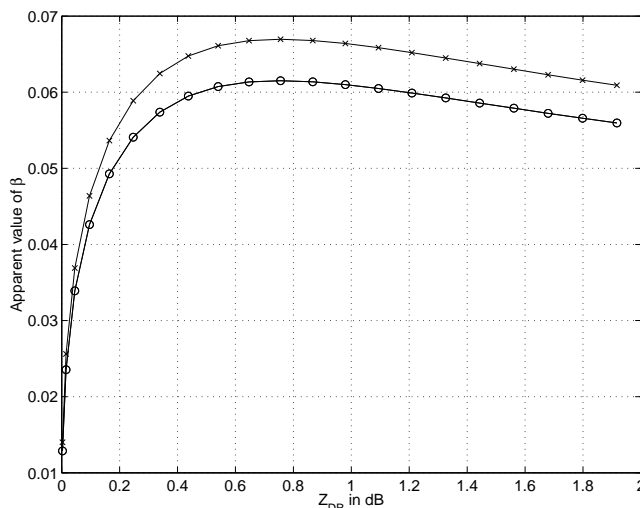


**Fig. 12.** The apparent value of  $\beta$  as a function of  $Z_{DR}$  if the rain drop spectrum is described as a normalised gamma function with  $\mu = 5$  (lower curve (o)). In the heavier rain  $D_0$ , and hence  $Z_{DR}$ , increases and leads to an apparent fall in  $\beta$ . The upper curve (x) shows the change in apparent  $\beta$  if the  $Z$  calibration changes by 1dB.

- *Sensitivity to calibration.*

Because the redundancy is being used to fix  $\beta$  it is assumed that  $Z$  is perfectly calibrated by some independent means. An small error in  $Z$  calibration of 1dB, will change  $\beta$  by about 10% (Fig 12).

- *Drop shape model.*

The use of a single free variable  $\beta$  may not be sufficient to define the drop

shape model; the intercept is also a variable (see Fig 6) and the curve is not necessarily a straight line.

- *Sensitivity to noisy  $K_{DP}$ .*

This approach involves the implicit computation of  $K_{DP}$  from the observations with its associated uncertainty, rather than the approaches above which use the more accurate integrated phase shift.

#### 6.4 The ZPHI technique

The ‘ZPHI’ technique is described by Testud et al. (2000) and encouraging results at C-band in heavy tropical rainfall are reported by Le Bouar et al. (2001). This method uses the total phase shift,  $\Phi_{DP}$  recorded along a path along which  $Z$  is observed to provide a constraint and fix the value of ‘ $a$ ’ in the  $Z = aR^b$  relationship. We now describe the principle of the technique at non-attenuating wavelengths such as S-band. At shorter wavelengths, C-band and below, attenuation can be appreciable, and the full technique which also uses the phase shift to correct for the attenuation is described in Testud et al. (2003, this book). In Section 3.4 it was shown that if naturally occurring raindrop spectra can be described by normalised gamma function then the value of  $b$  should be 1.5. Recall Eqn 12:

$$\frac{Z}{N_w} = H(\mu) \left( \frac{R}{N_w} \right)^{7.67/4.67} = H(\mu) \left( \frac{R}{N_w} \right)^b. \quad (24)$$

Fig. 13 shows that, for a normalised gamma function, a log-log plot of  $K_{DP}/N_w$  against  $Z/N_w$  with varying  $D_0$  is also very nearly a straight line which is only weakly dependent upon  $\mu$ . Thus, with we may write:

$$K_{DP}/N_w = f(Z/N_w)^g \quad \text{or} \quad K_{DP} = fN_w^{1-g}Z^g \quad (25)$$

where  $f$  and  $g$  are constants. Integrating along the path,  $r$ , we have:

$$\Phi_{DP} = fN_w^{1-g} \int Z^g dr \quad (26)$$

Accordingly, since  $f$  and  $g$  are known (Fig. 13) the value of  $N_w$  in Eqn 26 can be derived from the observed total phase shift,  $\Phi_{DP}$  and the path integral of the reflectivity raised to the power ‘ $g$ ’; the value of  $N_w$  then fixes ‘ $a$ ’ in  $Z = aR^{1.5}$ . Le Boar et al. (2001) report much improved rainfall rates at C-band, both as a result of the attenuation correction and from using the appropriate values of  $N_w$ . The technique has the following characteristics:

- *The total phase shift is a robust observation*

As for the calibration method described above, the technique avoids the use of a noisy value of  $K_{DP}$  obtained by differentiating the  $\phi_{DP}$  phase profile, but instead reduces the noise by integration. Note the sensitivity to the drop shape model. For the new drop shapes, when  $Z_H/N_W$  is below 1 (e.g.  $Z = 39\text{dBZ}$  and  $N_W = 8000 \text{ m}^{-3} \text{ mm}^{-1}$ ),  $g$  increases and approaches unity, but this region does not correspond to the regions of heavy rainfall with large phase shifts.

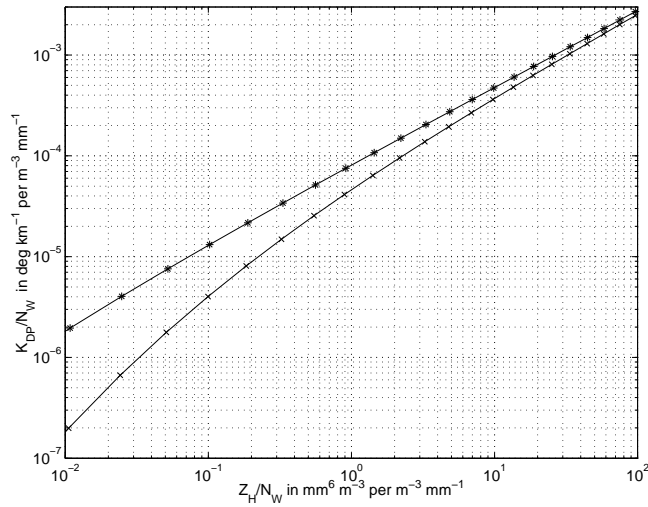


**Fig. 13.**  $K_{DP}/N_W$  for rain at S-band as a function of  $Z_H/N_W$  for a normalised gamma function with  $\mu=5$ : 'x' - New shapes. '\*' - Linear shapes. The ZPHI technique relies on this curve being a straight line with constant slope 'g' which is not unity.

- *Need for accurate calibration of Z*  
Any calibration error in  $Z$  will directly affect the derived value of  $N_w$  and the value of 'a' in the  $Z = aR^b$  relationship. Le Bouar et al. (2001) suggest that the method can be used to calibrate  $Z$ , based on the 'climatological' stability of  $N_w$ . They also propose a calibration technique which relies on the consistency of deriving rainfall rate from 'ZPHI' and from an attenuation corrected  $Z_{DR}$  and the inferred attenuation coefficient; in other words the method exploits the integrated phase information,  $Z_{DR}$  and  $Z$ , and is equivalent to the calibration techniques in Section 6.2 in another guise.
- *Sensitivity and operation in moderate rain rates*  
At C-band  $\Phi_{DP}$  must be above  $6^\circ$  at C-band if R is to be estimated to 32% and above  $32^\circ$  for 21% error. At this frequency  $10 \text{ mm hr}^{-1}$  has a one way  $K_{DP}$  of  $0.2^\circ \text{ km}^{-1}$  which would need to extend over 15km to produce a total differential phase shift of  $6^\circ$ . For  $50 \text{ mm hr}^{-1}$  the distance would be 2km, and for  $3 \text{ mm hr}^{-1}$  75km. All distances need to be multiplied by 5 to reduce the rainfall error to 21%.
- *Constraint of constant  $N_w$  along the path*  
This is quite restrictive, but the path may be divided into segments provided the total differential phase change per segment is at least  $6^\circ$ .
- *Interference from hail*  
A means of recognising hail is needed, otherwise hail will increase  $Z$  but not affect  $\Phi_{DP}$  and so lead to errors in inferred values of  $N_w$ .

The ZPHI technique is clearly a very powerful constraint for providing accurate rainfall rates in heavy rain. It is particularly applicable to the tropics where

hail is most unlikely. Based on the results of Matrosov et al. (1999) there is scope for extending the ZPHI technique to X-band for moderate rain rates.

## 7 Improved Rainfall Rates when Ice may be Present

In this Section we will consider two situations when the radar beam may be scanning a region containing icy hydrometeors. Firstly, in the summer time hail in convective clouds can occur at lower levels where the temperature is above freezing. Secondly, in the winter time and at longer ranges in all seasons the beam will be dwelling regions above the freezing level and can expect to encounter ice. In many papers only the first situation is addressed (e.g. Brandes et al., 1999) but at 200km range even in the summer the lowest elevation beam of a NEXRAD radar will be sampling ice.

### 7.1 Estimating rainfall when hail may be present

Apart from the use of  $K_{DP}$  alone, the techniques described in Section 6 for estimating rainfall rely upon an independent means of identifying the presence of hail. Hail cannot be identified unambiguously from the observed values of  $Z$  and  $Z_{DR}$ , but its presence will raise  $Z$  and depress  $Z_{DR}$ . The calibration technique of Goddard et al. (1994) relies on the consistency of the observed values of  $Z$ ,  $Z_{DR}$  at each gate and the total observed phase shift  $\Phi_{DP}$  along each ray within rain. Smyth et al. (1999) took this argument one stage further, suggesting that the best technique to identify hail is to continually monitor these three variables along each ray, and use the failure of the consistency as an indication of the presence of hail. When hail is present then the only approach is to use one of the  $R(K_{DP})$  equations to estimate the rainfall.

### 7.2 Estimating rainfall when the beam is at or above the freezing level

Essentially we are dealing with the problem of correcting for the vertical profile of reflectivity. This is a major operational problem and is dealt with in this book by Germann and Joss for mountainous regions and by Koistinen et al. for a cold climate. Can polarisation help in this problem? We must distinguish between the stratiform case, when there is an enhanced reflectivity,  $\Delta Z$ , of up to 10dB to 13dB associated with the melting of low density snowflakes and a rapid fall off of reflectivity in the ice above the bright band, and the convective case, when the higher density graupel particles are not associated with a bright band and the fall of reflectivity with height is less pronounced.

The bright band can easily be identified by its very obvious polarimetric signature; the values of LDR are generally in the range  $-14$  to  $-18$ dB and far higher than that of other precipitation particles. The enhanced value of  $Z$  in such regions,  $\Delta Z$  is about 10dB higher than in the rain below. Melting graupel is associated with lower values of LDR of about  $-22$  to  $-26$ dB and values of

Z similar to that in the rain below ( $\Delta Z=0\text{dB}$ ). This suggests that the value of LDR measured at the height of the  $0^\circ$  isotherm (obtained with an accuracy of  $1^\circ$  or so from an operational model) can be used as the basis of a bright band correction system. Before this is done the following aspects must be addressed:

- *Is there a reliable relationship between the LDR value and  $\Delta Z$ ?*  
How reliable is it and what is the quantitative performance of a Z correction scheme based on it?
- *Effect of range on the observed bright band*  
The bright band is typically about 600m deep and so at larger ranges will not fill the beam of a  $1^\circ$  radar. This means that the observed  $\Delta Z$  will be less. LDR should also be lower, but how well related are the two variables?
- *Absence of a bright band in convection*  
How reliable is the value of LDR which indicates the presence of graupel, and the absence of a bright band?
- *Propagation effects at C-band*  
As the beam propagates through regions of finite LDR, the targets depolarise the incident beam, and the apparent value of LDR rises with range. The effect is negligible at S-band but needs to be quantified at C-band. Is a correction scheme needed at C-band and can one be developed?

Deriving rainfall at the ground once the radar beam is dwelling only in the dry ice above the melting layer is a challenging problem which is very important for operational radars at most ranges in the cold season and for cold climates as extensively discussed in this book by Koistinen et al. The snow occurring at these heights does not have any very marked polarisation characteristics which can be exploited.

## 8 Correction for Attenuation

Gate by gate correction schemes are notoriously unstable (Hitschfeld and Borden, 1978) and very sensitive to small calibration errors (Hildebrand, 1978). Differential phase shift provides a very powerful technique to correct for attenuation. In heavy rain attenuation at C-band is a severe problem and affects both  $Z$  and  $Z_{DR}$ . For example, at  $40 \text{ mm hr}^{-1}$ , the attenuation,  $A_H$ , is about  $0.5 \text{ dB km}^{-1}$  and the differential attenuation,  $A_{DP}$ , is about  $0.1 \text{ dB km}^{-1}$ . In the literature there are many expressions of the form

$$A_H = \alpha K_{DP}^b \quad (27)$$

and

$$A_{DP} = \beta K_{DP}^b. \quad (28)$$

In the Rayleigh limit  $A_H$  is proportional to LWC (liquid water content) and for drop shapes which vary linearly with size,  $K_{DP}$  is proportional to the product of LWC and  $D_0$ , so at S-Band the value of 'b' in Eqn 27 is about 0.84. At C-band, the larger drops Mie scatter and absorb more, so that Eqn 27 is very

nearly linear. This suggests that correction for attenuation using  $K_{DP}$  or  $\Phi_{DP}$  at C-band should be reasonably straightforward. In practice the following factors need to be considered.

- *Temperature effects.*  
Attenuation depends upon the imaginary part of the dielectric constant which changes with temperature, but  $K_{DP}$  is a function of the real part which is constant. Attenuation is about twice as large at 0°C than at 20°C. Operational models provide a reliable temperature structure so, in principle, this effect can be corrected for.
- *The precise value of  $\alpha$  and  $\beta$  is a matter of some dispute.*  
Bringi et al. (1990) quote 0.054 and 0.0157 dB °C<sup>-1</sup>, respectively, at 15°C, but Carey et al. (2000) find that reported values range over a factor of two.
- *Variation with  $D_0$ .*  
Changes in the value of  $D_0$ , and hence the degree of Mie scattering, are probably the cause of this spread (Smyth and Illingworth, 1998; Carey et al., 2000). One method of resolving this difficulty would be an iterative approach, whereby the attenuation-corrected value of  $Z_{DR}$  is used to estimate  $D_0$  and hence the correct value of  $\alpha$  and  $\beta$ .

Our aim is to correct attenuations or  $Z$  to 1dB and  $Z_{DR}$  to 0.2dB (or better), so clearly, a quite complex attenuation correction is needed in the heaviest rain. There are two alleviating factors. In heavy attenuating rain, the value of  $\Phi_{DP}$  is large and it may be possible to use the ‘ZPHI’ method to correct for  $Z$  and avoid the more stringent requirement for correcting  $Z_{DR}$ . Smyth and Illingworth (1999) suggested using an additional constraint; the value of  $Z_{DR}$  on the far side of a storm where  $Z$  is low should be close to 0dB. Any negative values of  $Z_{DR}$  provide a path integrated constraint for the total path integrated value of  $A_{DP}$ .  $A_H$  (the total path attenuation) can then be derived from  $A_{DP}$  through a simple multiplicative factor, because both have the same temperature dependence. Bringi et al. (2001b) have combined these two constraints,  $\Phi_{DP}$  and  $Z_{DR}$  on the far side of the rain cell, so that the uncertain values of  $\alpha$  and  $\beta$  in Eqns 27 and 28 are no longer prescribed but are derived along with values of  $D_0$ ; the results are remarkably good and the technique is confirmed by the agreement with disdrometer values of  $D_0$ .

## 9 Identification of Hydrometeors

Thus far we have discussed identification of hydrometeors in terms of hail and melting snow impacting upon rainfall estimation. Hydrometeor identification itself is important for identifying severe weather (hail), for evaluation of the representation of different hydrometeors both in NWP models and in cloud resolving models (CRMs) and ultimately for assimilating hydrometeor information into such models. Particle classification also leads to a deeper understanding of the processes involved in precipitation formation and growth, so that conceptual

and numerical models can be improved. This is especially important in understanding deep convective systems as discussed in this book by Meischner et al. Straka et al. (2000) provide a very thorough review of the range of values in  $Z$ ,  $Z_{DR}$ ,  $K_{DP}$ , LDR and  $\rho_{HV}$  expected for hail, graupel, rain, rain wet hail mixtures, and snow crystals and aggregates. For example, hail can be identified by its high value of  $Z$  which is accompanied by lower values of  $Z_{DR}$  and  $K_{DP}$  than would be expected for rain. Liu and Chandrasekar (2000) have extended this classification using a fuzzy logic scheme; the in-situ validation data are very encouraging.

One difficulty that remains is that of identifying different forms of ice crystals. Matrosov et al. (2001) analysed the variation of the depolarisation ratio with elevation angle in terms of the ice particle aspect ratio and found the use quasi-circular polarisation provided the best discrimination. In theory pristine crystals have high density and so should give distinctive polarisation signatures. However, from an extensive analysis of in-situ data in stratiform clouds, Korolev et al. (2000) concluded that pristine crystals were rare and that 85% of ice particles were of irregular form. The problem is that the occasional large low density aggregates, which look spherical to the radar, dominate the radar return and mask the returns from the smaller crystals. This is confirmed by Wolde and Vali (2001) who found that in theory different crystal habits could be distinguished using a 94GHz polarimetric cloud radar, but that for real clouds polarimetric signatures were found for only a very few per cent of observations. Ryzhkov et al. (1998) suggested that the IWC should be related to a function of  $K_{DP}/Z_{DR}$  which should be insensitive to particle shape. Results were encouraging for regions containing pristine crystals, but the difficulty is that in the more common regions of aggregates, the values of the parameters are low and noisy and the IWC function is ill-defined. There is some scope for identifying ice particles by their signatures when they melt; for example, pristine plates will give very high  $Z_{DR}$  when they get wet, but after falling 100m or so will melt completely. We conclude that the polarimetric radar properties can be used to identify the larger hydrometeors but are usually unable to differentiate between the smaller types of ice particles.

## 10 Conclusion

This review has identified some powerful techniques based upon polarimetric observations. In the following discussion we shall assume that 'new' raindrop shapes of Eqn 5 are accurate, and that natural raindrop size spectra can be represented by a normalised gamma function with a mean shape factor of 5 and a range of 1-10, and an average normalised concentration  $N_w$  of  $8000 \text{ m}^{-3} \text{ mm}^{-1}$  with a range of up to a factor of ten both larger and smaller. This range leads to a relationship of the form  $Z = aR^{1.5}$  with 'a' proportional to  $1/\sqrt{N_w}$  and errors of up to a factor of two in rain rate. If we are to estimate rainfall rates to better than 25%, then it may be necessary to account for the increased terminal velocities ( $\approx 10\%$  at 2km) aloft (Matrosov et al., 2002).

- *Ground clutter and anomalous propagation*  
They can be recognised at each gate using polarimetric parameters. Particularly powerful is the use of the copolar correlation coefficient as a data quality check.
- *Rain rates from  $Z$  and  $Z_{DR}$*   
 $Z$  should scale with  $R$  as for a given  $Z_{DR}$  (or  $D_0$ ) as  $N_w$  changes; this leads to a formula of the form  $Z/R = f(Z_{DR})$  given by Eqn 14 at S-band and 15 at C-band. For rainrates to be accurate to 25%,  $Z$  must be calibrated to better than 25% (1dB).  $Z_{DR}$  must be accurate to 0.2dB for  $R > 10\text{mm hr}^{-1}$  and 0.1dB for  $R > 3\text{mm hr}^{-1}$ . Such  $Z_{DR}$  accuracies are difficult to achieve in practice on a scale of 2km.
- *Rain rate from  $K_{DP}$*   
This technique is attractive because of its immunity to both calibration errors and to attenuation and to its insensitivity to hail. However, the exponent in  $K_{DP} = aR^b$  is about 1.4 and not very different from those in  $Z - R$  relations, so the  $R$  derived from  $K_{DP}$  has almost the same sensitivity to changes in raindrop spectra as  $R$  derived from  $Z$ , and the scope for using path integrated phase shift to infer rainfall over a catchment is limited. In addition, the differential phase measurement is inherently noisy and in practice is also extremely sensitive to small amounts of ground clutter or mismatched sidelobe signals. As a result the  $R$  estimates from  $K_{DP}$  are not accurate enough for operational work at 2km resolution unless hail is present.
- *Use of integrated polarisation parameters*  
We conclude that at the 2km scale needed for an operational system, the additional information from  $Z_{DR}$  and  $K_{DP}$  is insufficiently accurate to improve rainfall estimates, but that the use of integrated polarisation parameters can provide a valuable constraint.
- *Auto-calibration of  $Z$  and identification of hail*  
 $Z$  can be accurately calibrated to 0.5dB (10%) by exploiting the fact that  $Z_{DR}$  and  $K_{DP}$  are not independent in rain, but that  $K_{DP}/Z$  is a unique function of  $Z_{DR}$ . The technique is to compute the predicted total theoretical differential phase shift along a ray ( $\Phi_{DP}$ ), by integrating the value of  $K_{DP}$  predicted from the observed values of  $Z$  and  $Z_{DR}$  at each gate, and then scaling the  $Z$  values so that the predicted value of  $\Phi_{DP}$  agrees with the observed one. This technique avoids using the noisy observed  $K_{DP}$ . The presence of hail can be inferred from the failure of the redundancy exploited in the calibration technique.
- *Drops shape constraint from polarisation redundancy?*  
An alternative approach is to exploit this redundancy by choosing the value of  $\beta$  in the drop shape (Eqn 4) so that the observed  $Z$ ,  $Z_{DR}$  and  $K_{DP}$  are consistent, but the accuracy is limited because this approach uses the very noisy observed values of  $K_{DP}$ . It seems more sensible to accept the extensive measurements of drop shape and use the redundancy to fix the  $Z$  calibration.
- *The ‘ZPHI’ technique to fix ‘a’ in  $Z = aR^{1.5}$  in heavy rain*  
The observed path integrated differential phase shift,  $\Phi_{DP}$ , together with the integrated value of  $Z$  along the ray can be used in the ‘ZPHI’ technique



to provide a constraint to  $N_w$  and hence an estimate of ‘ $a$ ’ in  $Z = aR^{1.5}$  provided there is no hail present. The technique is limited to rather heavy rainfall because  $\Phi_{DP}$  at C-band must be at least  $32^\circ$  if the error in  $R$  is to be reduced to 21%. Increased phase shifts at X-band may be counteracted by the extra noise introduced by Mie scattering effects, such as differential phase shift on backscatter and a lowering of the co-polar correlation coefficient.

- *Use of  $\phi_{DP}$  to correct  $Z$  and  $Z_{DR}$  for attenuation*  
 $\phi_{DP}$  is nearly linearly related to attenuation at C-band but the constant changes with  $T$  and  $D_0$ . Correction of attenuation using the ‘ZPHI’ technique is discussed by Testud et al. (2003, this book). Further improvements to the attenuation correction may be possible when the ‘ZPHI’  $\Phi_{DP}$  constraint is combined with the requirement that the total differential attenuation is consistent with the values of  $Z_{DR}$  expected on the far side of a heavy rain echo. There is scope for using the ZPHI method at X-band (3.2cm) provided the rainfall is not too heavy so there is total loss of signal.
- *Integrated  $Z/Z_{DR}$  technique in regions of low rainfall*  
 In regions of moderate or light rain where the phase shifts are too low for the ZPHI technique, the average value of  $N_w$  over a domain can be inferred from the many estimates of  $N_w$  from  $Z$  and  $Z_{DR}$  made at each gate. The random errors associated with noisy  $Z_{DR}$  should average to zero, and providing  $Z$  is accurately calibrated, the mean value of  $N_w$  can be estimated, and hence accurate (25%) rainfall estimates obtained down to perhaps  $R = 3 \text{ mm hr}^{-1}$ , but this still remains to be demonstrated.
- *Hydrometeor Identification*  
 Combined polarisation parameters can be used to distinguish the different types of the larger hydrometeors and this should be useful in evaluating parameterisation schemes in NWP (Numerical Weather Prediction) models and the performance of CRMs (Cloud Resolving Models), and may ultimately be used for assimilation into such models (see Macpherson et al., 2003, this book).

To summarise, we find that polarisation radar has the potential to remove most of the ambiguities which arise when  $Z$  alone is measured with a conventional radar. However, the difficulty of estimating rainfall rates at the ground at long ranges when the beam is dwelling in ice above the melting layer remains. In all these applications it is important to use the latest ‘new’ raindrop shapes. It may be that the use of the ‘linear’ drop shapes is responsible for some of the disappointing rainfall estimates reported in the literature. The requirement for pulse to pulse switching of polarisation can be avoided by the use of ‘hybrid’ ( $45^\circ$ ) transmission, but this approach will probably not reduce the noise of the differential phase measurement. Ground clutter and ‘anaprop’ can be unambiguously recognised, but generally, the parameters cannot be estimated accurately enough to contribute independent information to improve rainfall estimates on the operational scale of 2km. However, when the parameters are integrated over a domain, they can correct for attenuation in C-band systems, provide absolute calibration of  $Z$  to 10%, and reduce errors in inferred rainfall rates from

a factor of two down to about 25%, effectively by fixing the value of ‘ $a$ ’ to be used in  $Z = aR^{1.5}$  over a domain. Finally, to accompany these improved rainfall estimates the polarisation parameters can also provide an estimate of the error which is essential for use in data assimilation.

## References

1. Andsager, K., K.V.Beard and N.F.Laird, 1999: Laboratory measurements of axis-ratios for large raindrops. *J. Atmos. Sci.*, 56, 2673-2683.
2. Battan, L.J., 1973: *Radar Observations of the Atmosphere*. University of Chicago Press, 324pp.
3. Blackman, T.M and A.J.Illingworth, 1995: Improved measurements of rainfall using differential phase techniques. COST 75 Int Seminar on Weather Radar Systems, ed C.G.Collier, EUR 16013 EN.
4. Blackman, T.M. and A.J.Illingworth, 1997: Examining the lower limit of  $K_{DP}$  rainrate estimation including a case study at S-band. Preprints 28th Int. Conf. on Radar Meteor., Amer. Meteor. Soc.
5. Brandes, E.A., J.Vivekanandan and J.W.Wilson, 1999: A comparison of radar reflectivity estimates from collocated radars. *J. Atmos. Oceanic Technol.*, 16, 1264-1272.
6. Brandes, E.A., A.V.Ryzhkov and D.S.Zrnich, 2001: An evaluation of radar rainfall estimates from specific differential phase. *J. Atmos. Oceanic Technol.*, 18, 363-375.
7. Bringi, V.N., T.A.Seliga and S.M.Cherry, 1983: Statistical properties of the dual-polarization differential reflectivity ( $Z_{DR}$ ) signal. *IEEE Trans. Geosci. Remote Sens.*, 21, 215-220.
8. Bringi, V.N., V.Chandrasekar, N.Balakrishnan, and D.S.Zrnich, 1990: An examination of propagation effects in rainfall on radar measurements at microwave frequencies. *J. Atmos. Oceanic Technol.*, 7, 829-840.
9. Bringi, V.N., Gwo-Jong Huang, V. Chandrasekar and T.D.Keenen, 2001a: An areal rainfall estimator using differential propagation phase; Evaluation using a C-band radar and a dense gauge network in the tropics. *J. Atmos. Oceanic Technol.*, 18, 1810-1818.
10. Bringi, V.N., T.D.Keenen and V. Chandrasekar, 2001b: Correcting C-band radar reflectivity and differential reflectivity data from rain attenuation: A self consistent method with constraints. *IEEE Trans. Geosci. Remote Sens.*, 39, 1906-1915.
11. Bringi V N and V Chandrasekar, 2001: *Polarimetric Doppler weather radar*. CUP, 636pp.
12. Carey, L.D., S.A.Rutledge, D.A.Ahijevych and T.D.Keenan, 2000: Correcting propagation effects in C-band polarimetric radar observations of tropical convection using differential propagation phase. *J. Appl. Meteor.*, 39, 1405-1433.
13. Caylor, I.J. and A.J.Illingworth, 1992: ‘Polarisation radar estimates of rainfall; correction of errors due to the bright band and to anomalous propagation’ *International Weather Radar Networking*, pp332 Kluwer, Dordrecht.
14. Chandrasekar, V. and V.N.Bringi, 1988a: Error structure of multiparameter radar and surface measurement of rainfall. Part 1: Differential Reflectivity. *J. Atmos. Oceanic Technol.*, 5, 783-795.
15. Chandrasekar, V. and V.N.Bringi, 1998b: Error structure of multiparameter radar and surface measurement of rainfall. Part II: X-band attenuation. *J. Atmos. Oceanic Technol.*, 5, 796-802.

16. Chandrasekar, V., V.N.Bringi, N.Balakrishnan and D.S.Zrnic, 1990: Error structure of multiparameter radar and surface measurement of rainfall. Part III: Specific differential phase. *J. Atmos. Oceanic Technol.*, 7, 621-629.
17. Frost, I.R., J.W.F.Goddard and A.J.Illingworth, 1991: Hydrometeor identification using cross polar radar measurement and aircraft verification. Preprints 25th Int. Conf. on Radar Meteor., Amer. Meteor. Soc.
18. Goddard, J.W.F., S.M.Cherry and V.N.Bringi, 1982: Comparison of dual-polarization radar measurements of rain with ground based disdrometer measurements. *J. Appl. Meteor.*, 21, 252-256.
19. Goddard, J.W.F., J.Tan and M.Thurai, 1994: Technique for calibration of meteorological radars using differential phase. *Electronics Letters*, 30, 166-167.
20. Goddard, J.W.F, K.L.Morgan, A.J.Illingworth and H.Sauvageot, 1995: Dual-wavelength polarisation measurements in precipitation using the CAMRA and Rabalais radar. Preprints 27th Int. Conf. on Radar Meteor., Amer. Meteor. Soc.
21. Gorgucci, E., G.Scarchilli and V.Chandrasekar, 1994: A robust estimator of rainfall rate using differential reflectivity. *J. Atmos. Oceanic Technol.*, 11, 586-592.
22. Gorgucci, E., G.Scarchilli and V.Chandrasekar, 1999a: Specific differential phase estimation in the presence of nonuniform rainfall medium along the path. *J. Atmos. Oceanic Technol.*, 16, 1690-1697.
23. Gorgucci, E., G.Scarchilli and V.Chandrasekar, 1999b: A procedure to calibrate multiparameter weather radar using properties of the rain medium. *IEEE Trans. Geosci. Remote Sens.*, 17, 269-276.
24. Gorgucci, E., G.Scarchilli, V.Chandrasekar and V.N.Bringi, 2000: Measurement of mean raindrop shape from polarimetric radar observations. *J. Atmos. Sci.*, 57, 3406-3413.
25. Gorgucci, E., G.Scarchilli, V.Chandrasekar, and V.N.Bringi, 2001: Rainfall estimation from polarimetric radar measurements: Composite algorithms immune to variability in raindrop shape-size relation. *J. Atmos. Oceanic Technol.*, 18, 1773-1786.
26. Hagen, M., 1997: Identification of ground clutter by polarimetric radar, Preprints 28th Int. Conf. on Radar Meteor., Amer. Meteor. Soc.
27. Hall, M.P.M., J.W.F.Goddard and S.M.Cherry, 1984: Identification of hydrometeors and other targets by dual-polarization radar. *Radio Sci.*, 19, 132-140.
28. Herzegh, P.H. and R.E.Carbone, 1984: The influence of antenna illumination function characteristics on differential reflectivity measurements. Preprints 22nd Int. Conf. on Radar Meteor., Amer. Meteor. Soc.
29. Hildebrand, P.H., 1978: Iteritive correction for attenuation of 5cm radar in rain. *J. Appl. Meteorol.*, 17, 508-514.
30. Hitschfeld, W., and J. Bordan, 1954: Errors inherent in the radar measurement of rainfall at attenuating wavelengths. *J. Meteorol.*, 11, 58-67.
31. Hubbert, J., V.Chandrasekar, V.N.Bringi, and P.F.Meischnr, 1993: Processing and interpretation of coherent dual-polarized radar measurements,. *J.Atmos. Oceanic Technol.*, 10, 155-164.
32. Hubbert, J., and V. N. Bringi, 2000: The effects of three-body scattering on differential reflectivity signatures. *J. Atmos. Oceanic Technol.*, 17, 51-61.
33. Illingworth, A.J., J.W.F.Goddard and S.M.Cherry, 1987: Polarisation radar studies of precipitation development in convective storms. *Q. J. R. Meteorol. Soc.*, 113, 469-489.
34. Illingworth, A.J. and I.J.Caylor, 1988: Identification of precipitation particles using dual polarization radar. 10th Int Conf on Cloud Physics, Bad Hamburg, Germany.
35. Illingworth, A.J. and I.J.Caylor, 1991: Co-polar correlation measurements of precipitation. Preprints 25th Int. Conf. on Radar Meteor., Amer. Meteor. Soc.

36. Illingworth, A.J. and T.M.Blackman, 1999: The need to normalise RSDs based on the gamma RSD formulation and implications for interpreting polarimetric radar data. Preprints 29th Int. Conf. on Radar Meteor., Amer. Meteor. Soc.
37. Illingworth, A.J. and M.P.Johnson, 1999: The role of raindrop shape and size spectra in deriving rainfall rates using polarisation radar. Preprints 29th Int. Conf. on Radar Meteor., Amer. Meteor. Soc.
38. Illingworth, A.J., and T.M.Blackman, 2002: The need to represent raindrop size spectra as normalized gamma distributions for the interpretation of polarization radar observations. *J. Appl. Meteor.*, 41, 1578-1583.
39. Keenan, T., K.Glasson, F.Cummings, T.S.Bird, J.Keeler and J.Lutz, 1998: The BMRC/NCAR C-band Polarimetric (C-POL) Radar System. *J. Atmos. Oceanic Technol.*, 15, 871-886.
40. Korolev, A., G.A.Isaac and J.Hallett, 2000: Ice particle habits in stratiform clouds. *Q. J. R. Meteorol. Soc.*, 126, 2873-2902.
41. Kozu.,T. and K.Nakamura, 1991: Rainfall parameter estimation from dual-radar measurements combining reflectivity profile and path-integrated attenuation. *J. Atmos. Oceanic Technol.*, 8, 259-271.
42. Le Bouar, E., J.Testud, T.D.Keenan, 2001: Validation of the rain profiling algorithm 'ZPHI' from the C-band polarimetric weather radar in Darwin. *J. Atmos. Oceanic Technol.*, 18, 1819-1837.
43. Liu, H.P. and V.Chandrasekar, 2000: Classification of hydrometeors based on polarimetric radar measurements: Development of fuzzy logic and neuro-fuzzy systems, and in situ verification. *J. Atmos. Oceanic Technol.*, 17, 140-164.
44. Marshall, J.S. and W.M.K.Palmer, 1948: The distribution of raindrops with size. *J. Meteor.*, 5, 165-166.
45. Matrosov, S.Y., R.A.Kropfli, R.F.Reinking and B.E.Martner, 1999: Prospects for measuring rainfall using propagation differential phase in X- and Ka- radar bands. *J. Appl. Meteor.*, 38, 766-776.
46. Matrosov,S.Y., R.F.Reinking, R.A.Kropfli, B.E.Martner and B.W.Bartram, 2001: On the use of radar depolarization ratio for estimating shape of ice hydrometeors in winter clouds. *J. Appl. Meteor.*, 40, 479-490.
47. Matrosov, S.Y., K.A.Clark, B.E.Martner and A Tokay, 2002: X-band polarimetric radar measurements of rainfall. *J. Appl. Meteor.*, 41, 941-952.
48. May,P.T., T.D.Keenan, D.S.Zrnic, L.D.Carey and S.A.Rutledge, 1999: Polarimetric radar measurements of tropical rain at 5-cm wavelength. *J. Appl. Meteor.*, 38, 750-765.
49. Pamment, J.A. and B.J.Conway, 1994: Objective identification of echoes due to anomalous propagation in weather radar. *J. Atmos. Oceanic Technol.*, 15, 98-113.
50. Petersen,W.A., L.D.Carey, S.A.Rutledge, J.C.Knievel, N.J.Doesken, R.H.Johnson, T.B.McKee, T.Vonder Haar, and J.F.Weaver, 1999: Mesoscale and radar observations of the Fort Collins flash flood of 28 July 1997. *Bull. Amer. Meteorol. Soc.*, 80, 191-216.
51. Pruppacher, H.R. and R.L.Pitter,1971: A semi-empirical determination of the shape of cloud and raindrops. *J. Atmos. Sci*, 28, 86-94.
52. Ryzhkov, A.V. and D.S.Zrnic, 1995: Comparison of dual-polarisation radar estimators of rain. *J. Atmos. Oceanic Technol.*, 12, 249-256.
53. Ryzhkov, A.V. and D.S.Zrnic, 1996: Assessment of rainfall measurement that uses specific differential phase. *J. Appl. Met.*, 35, 2080-2090.
54. Ryzhkov, A.V. and D.S.Zrnic, 1998a: Beamwidth effects on the differential phase measurement of rain. *J. Atmos. Oceanic Technol.*, 15, 624-634.

55. Ryzhkov, A.V. and D.S.Zrnica, 1998b: Polarimetric rainfall estimation in the presence of anomalous propagation. *J. Atmos. Oceanic Technol.*, 15, 1320-1330.
56. Ryzhkov, A.V., D.S.Zrnica and B.A.Gordon, 1998: Polarimetric method for ice water content determination. *J. Appl. Meteor.*, 37, 125-134.
57. Ryzhkov, A.V., D.S.Zrnica and R.Fulton, 2000: Areal rainfall estimates using differential phase. *J. Appl. Meteor.*, 39, 263-268.
58. Sachidananda, M. and D.S.Zrnica, 1986: Differential propagation phase shift and rainfall estimation, *Radio Sci.*, 21, 235-247.
59. Sachidananda, M. and D.S.Zrnica, 1987: Rain rate estimates from differential polarisation measurements. *J. Atmos. Oceanic Technol.*, 4, 588-598.
60. Seliga, T., and V.N.Bringi, 1976; Potential use of radar differential reflectivity measurements at orthogonal polarisations for measuring precipitation. *J. Appl. Meteor.*, 15, 69-75.
61. Smyth, T.J. and A.J.Illingworth, 1998: Correction for attenuation of radar reflectivity using polarisation data. *Q. J. R. Meteorol. Soc.*, 124, 2393-2415.
62. Smyth, T.J., T.M.Blackman and A.J.Illingworth, 1999: Observations of oblate hail using dual polarisation radar and implications for hail-detection schemes. *Q. J. R. Meteorol. Soc.*, 125, 993-1016.
63. Straka, J.M., D.S.Zrnica and A.V.Ryzhkov, 2000: Bulk hydrometeor classification and quantification using polarimetric radar data: Synthesis of Relations, *J. Appl. Meteor.*, 39, 1341-1372.
64. Testud, J., E.L.Bouar, E.Obligis, M.Ali-Mehenni, 2000: The rain profiling algorithm applied to polarimetric weather radar. *J. Atmos. Oceanic Technol.*, 17, 332-356.
65. Testud, J., S.Oury, R.A.Black, P.Amayenc, and D.Xiankang, 2001: The concept of 'normalized' distribution to describe raindrop spectra: A tool for cloud physics and cloud remote sensing. *J. Appl. Meteor.*, 40, 1118-1140.
66. Ulbrich, C.W., 1983: Natural variations in the analytical form of the raindrop size distribution. *J. Clim and Appl. Met.*, 22, 1764-1775.
67. Ulbrich, C.W. and D.Atlas, 1998: Rainfall microphysics and radar properties: analysis methods for drop size spectra. *J. Appl. Meteor.*, 37, 912-923.
68. Upton G and J-J Fernandez-Duran, 1999; Statistical techniques for clutter removal and attenuation detection in radar reflectivity Cost 75 Int. Seminar, Advanced Weather Radar Systems, Locarno, EUR 18567 EN. 858pp.
69. Wilson, D.R., A.J.Illingworth and T.M.Blackman, 1995: The use of Doppler and polarisation data to identify ground clutter and anaprop. Weather Radar Systems, ED C.G.Collier, Cost-75 EUR 16013 EN p527-538.
70. Wilson, D.R., A.J. Illingworth and T.M.Blackman, 1997: Differential Doppler Velocity: A radar parameter for characterising hydrometeor size distributions. *J. Appl. Meteor.*, 36, 649-663.
71. Wolde, M., and G. Vali, 2001: Polarimetric signatures from ice crystals observed at 95GHz in winter cloud. Part II: Frequency of occurrence. *J. Atmos. Sci.*, 58, 842-849.